New Smart Functional Fluorophores based on Stable Spirocyclic Zwitterionic Meisenheimer Compounds

Neus Sala,[a] Gemma Prats,[a,] Marc Villabona,[a] Iluminada Gallardo,[a] Tarafah Hamdan, [b]

Rabih O. Al-Kaysi,*[b] Jordi Hernando,*[a] and Gonzalo Guirado*[a]

[a] Departament de Química, Universitat Autònoma de Barcelona, 08193 Cerdanyola del Vallès, Spain

[b] College of Science and Health Professions-3124, King Saud bin Abdulaziz University for Health Sciences and King Abdullah International Medical Research Center, Ministry of National Guard Health Affairs, Riyadh 11426, Kingdom of Saudi Arabia

E-mails of corresponding authors: jordi.hernando@uab.cat (J.H.); rabihalkaysi@gmail.com and

kaysir@ksau-hs.edu.sa (R.O.K.); gonzalo.guirado@uab.cat (G.G.)

ABSTRACT. Molecules and materials showing stimulus-induced modulation of their optical properties are of interest in a large variety of areas. In this paper we focus on fluorescent switches based on stable spirocyclic zwitterionic Meisenheimer compounds (SZMC), which are composed of a 2,4,6-trisubstitued cyclohexadienyl anion chromophore fused with a triazene ring via a spiro carbon atom. By exploiting a facile one-pot synthetic strategy, new SZMC switches have been prepared with halo-, electro- and thermochromic properties. These properties can be controlled by modifying the substituents on their two constituting units. In particular, the optical properties, the sensitivity to different chemical stimuli, and the range of thermal response of these systems can be tailored by varying (a) the nature of the electron-withdrawing groups in their 2,4,6-trisubstitued cyclohexadienyl anion chromophore, and (b) the bulkiness of the pending chains in their triazene ring. In combination with their versatile optical switching behavior, this synthetic tunability makes SZMC switches very promising functional molecules for applications in chemistry, materials science and biosciences.

1. INTRODUCTION

Spirocyclic organic molecules are emerging as promising molecular architectures for the synthesis of novel anticancer [1,2] and antiinflamatory drugs [3] due to their resemblance to the 3D bond framework of natural products. Moreover, some spirocyclic compounds can be used in a broad range of materials science applications, such as in optoelectronics [4], photochromic systems [5–8], photoswitches to control the aggregation of nanoparticles [9,10], or as switchable fluorophores for sensing and imaging [11]. With several of these applications in mind, we have pioneered the development of a new family of fluorescent molecular switching systems based on stable spirocyclic zwitterionic Meisenheimer compounds (SZMC), which are composed of a 2,4,6-trisubstituted cyclohexadienyl anion chromophore linked to a triazene ring through a sp3 hybridized carbon atom (Scheme 1a) [12–16].

Two are the main advantages of SZMC fluorescent switches. Firstly, they can be prepared via a facile one-pot synthesis from readily available starting materials., which proceeds through the first steps of nucleophilic aromatic substitution reactions that lead to the formation of spirocyclic Meisenheimer complexes in the presence of electron withdrawing groups on the starting aromatic ring [17,18]. Secondly, they display versatile optical switching in response to different types of external stimuli. Thus, reversible interconversion between their non fluorescent anionic state (**1a-2a**) and highly fluorescent zwitterionic form (**1b-2b**) occurs both by acid-base addition and electrochemically (Scheme 1a) [15,19]. Furthermore, transformation of the anionic spirocyclic state of these compounds into a fluorescent species can also be realized by interaction with Lewis acids [15]. Finally, proper chemical functionalization of the cyclohexadienyl anion of SZMCs reduces the stability of their spirocyclic structure and enables reversible formation of a non colored and non fluorescent aromatic state (**2c**), which can be controlled thermally (Scheme 1a). As such, this allows the design of a three-state fluorescent molecular switch with halo-, electro- and thermochromic behavior [20].

These properties of SZMC fluorescent switches have so far been exploited in a variety of applications, such as in single molecule on/off fluorescence modulation [15] and for the preparation of molecular analogues of field effect transistors [20], stable luminescent nanoparticles [21], optical chemosensors of

F[-] and CN^{-} anions [22,23], ammonia [24] and explosives [25] as well as invisible security inks [24]. For many of these applications, proper selection of the substituents of both the 2,4,6-trisubstituted cyclohexadienyl anion chromophore and the triazene ring is required, since they ultimately control the performance of SZMC switches. Thus, replacement of the *para*-nitro group of the chromophore by a trifluoromethyl moiety red-shifts its absorption and emission spectra, and expands the sensitivity of the compound to thermal stimuli [20]. On the other hand, surrounding the guanidinium group of the triazene ring with either isopropyl or cyclohexyl groups drastically changes the response to weak bases such as CN^{-} ions for sensing purposes [22,23]. In view of this, the preparation and characterization of new SZMC switches **4b**, **5b** and **6b** is reported herein (Scheme 1b).
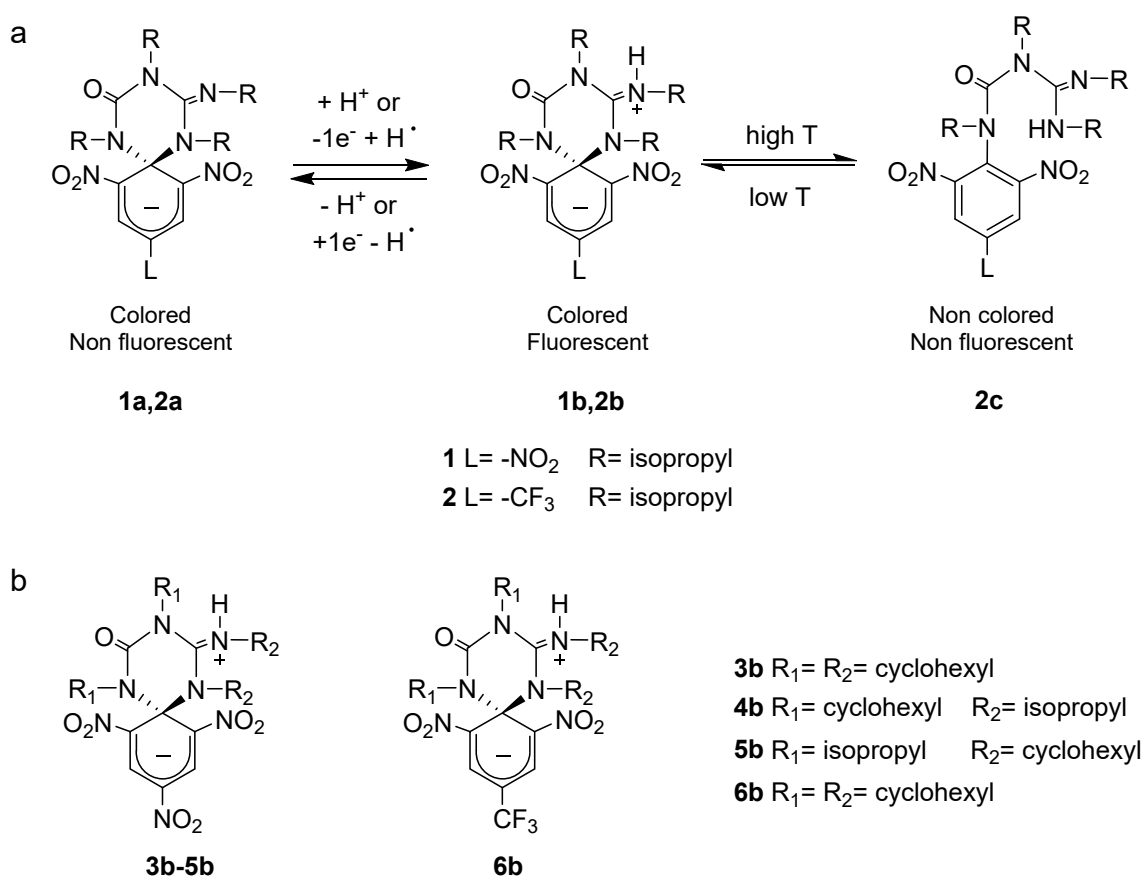
Scheme 1. (a) Multi-stimuli responsive behavior of SZMC switches **1b** [¡**Error! Marcador no definido.**-¡**Error! Marcador no definido.**] and **2b** [12]. (b) Structures of new potential SZMC switches **4b-6b**.

Although compound **3b** was previously reported by us [12,13,22] and others [24], a complete description of their switching behavior has not been reported yet.

2. EXPERIMENTAL SECTION

2.1. Materials and methods

Organic solvents used in the synthesis were distilled over CaH_2 and stored over activated molecular sieves (3 Å). Spectroscopic grade solvents were used as received. All chemicals used for the synthesis were of reagent grade with > 98% purity and they were used without further purification. Flash column chromatography was performed on silica gel 60 Å with average particle size 35-70 μm. ^1H NMR spectra were recorded on Bruker DPX250 (250 MHz), Bruker DPX360 (360 MHz) and Bruker AV-III400 (400 MHz) spectrometers. ^{13}C NMR spectra were recorded on a Bruker AV-III400 (100 MHz) spectrometer with complete proton decoupling. Proton chemical shifts are reported in ppm (δ) ($CDCl_3$, δ 7.26 ppm or CD_3CN, δ 1.94 ppm) and *J* values are reported in Hz. Carbon chemical shifts are reported in ppm (δ) ($CDCl_3$, δ 77.2 ppm or CD_3CN, δ 1.32 ppm) and *J* values are reported in Hz. High resolution mass spectra (HRMS) were recorded on an ESI-QTOF Bruker Daltonics microTOF-Q spectrometer.

2.2. Optical characterization

UV-vis absorption spectra were recorded using a HP 8452A spectrophotometer (Agilent) with Chemstation software. Fluorescence spectra were recorded by means of a custom-made spectrofluorometer using cw lasers (λ_{exc} = 473 nm; Z-laser, λ_{exc} = 532 nm) as excitation sources. Emitted photons were detected using an Andor ICCD camera coupled to a spectrograph. In all the cases spectroscopic quality solvents and 1-cm quartz cuvettes were used. Temperature was controlled using a refrigerated circulator bath (Huber MPC-K6) connected to the sample holder. Fluorescence quantum yields were determined for highly diluted solutions of the compounds of interest to prevent self-absorption processes (absorption < 0.05 at the excitation wavelength) and were measured relative to *N,N'*-bis(1-hexylheptyl)perylene-3,4,9,10 tetracarboxybismide in acetonitrile (Φ_f=1) [26] or *N,N'*-bis(butyl)-

1,6,7,12-tetra-(4-*tert*-butylphenoxy)perylene-3,4:9,10-tetracarboxylic diimide in CH_2Cl_2 (Φ_f =1) [27]. For anion chemosensing experiments, tetraethylammonium fluoride, tetraethylammonium cyanide, tetrabutylammonium chloride, tetrabutylammonium bromide and potassium iodide salts were used.

2.3. Electrochemical characterization and switching

Cyclic voltammograms were registered using a VSP100 BIOLOGIC potentiostat and a conical electrochemical cell equipped with an argon bubbling source for degassing, a glassy carbon working electrode (WE, d= 0.45 mm), a glassy carbon auxiliary electrode (CE, d= 3 mm) and a saturated calomel reference electrode (SCE, RE). All the potentials are reported versus a SCE isolated from the working electrode by a salt bridge. All measurements were performed in acetonitrile solution containing 0.1 M of *n*-Bu$_4$NPF$_6$ as a supporting electrolyte. Electrolysis experiments at controlled potentials were undertaken with a EG&G Princeton Applied Research (PAR) 273A potentiostat and an electrochemical cell equipped with an argon bubbling source, a carbon graphite rod, an auxiliary platinum electrode and a SCE reference electrode. All experiments were performed in acetonitrile solutions containing *n*-Bu$_4$NPF$_6$ (0.1 M) as a supporting electrolyte. The products obtained were then characterized by ^{1}H NMR, cyclic voltammetry, UV-Vis absorption spectroscopy and fluorescence spectroscopy.

Spectroelectrochemical experiments were performed in a thin layered quartz glass cell using a platinum gauze and a platinum wire as working and counter electrodes respectively, whereas a saturated calomel electrode (SCE) was used as a reference electrode. A computer-controlled VSP-potentiostat synchronized with an MMS-UV-Vis high speed diode array spectrometer with a bandwidth of 330–1100 nm and a deuterium/tungsten light source (HM) and optical fiber (SMA, J&M) was employed to register the spectroelectromical measurements. Each spectrum was recorded after 0.05 s. BioKine32 software was used for data acquisition and treatment.

2.4. Synthesis

SZMC switches **1b** [13, 14, 20], **2b** [20] and **3b** [22, 24] were synthesized as previously reported.

2.2.1. Synthesis of compounds **4b** and **5b**

A solution of picric acid (0.44 g, 1.91 mmol) in CH_2Cl_2 (5 mL) was quickly added to a chilled (5 ^{0}C) solution of *N,N'*-dicyclohexylcarbodiimide (0.39 g, 1.91 mmol) and *N,N'*-diisopropylcarbodiimide (0.24, 1.91 mmol) and a catalytic amount of 4-dimethylaminopyridine in CH_2Cl_2 (10 mL). The reaction was stirred under an argon atmosphere for 10 h while slowly brought back to room temperature. Unreacted picric acid was partially removed by washing the reaction mixture with aqueous $NaHCO_3$ solution (1 M). The organic layer was dried with anhydrous $MgSO_4$, then decanted, and the solvent removed under reduced pressure to yield a red glassy residue containing a mixture of **1b**, **3b**, **4b** and **5b** together with monosubstitution products **7** and **8** along with traces of the unreacted carbodiimides. The latter were removed upon sonication of the crude mixture with hexanes (10 mL) and decanting the diimide-free crude red powder. The crude product mixture (0.58 g) was separated by flash chromatography [28,29] (1:1 ethyl acetate: hexane). The eluted fractions were unambiguously identified by NMR analysis. Because of the difference in lipophilicity of cyclohexyl and isopropyl moieties as well as the effect of the alkyl substituents surrounding the protonated guanidinium NH^+ group that shield its interaction with the silica stationary phase, the distinct zwitterionic products were eluted in the following order: **3b** (46 mg, 4%), **5b** (35 mg, 3%), **4b** (52 mg, 5%), **1b** (50 mg, 5%) with a total combined yield of 17%. The yield of each fraction represents the experimental isolated yield. For a better purification of these products in view of fluorescence experiments, preparative TLC was also performed on the crude product using a 20 x 20 cm, 1 mm-thick silica gel TLC plate. A 5 mg sample of the crude product was dissolved in ethyl acetate and deposited onto the plate. Elution using the same mobile phase used for flash column chromatography allowed separation of the target products into four distinct bands that were carefully scrapped and extracted with equal amounts of acetonintrile (Fig. S1). Spectroscopic data for **1b** [12,13,22], **3b** [22,24], **7** [12] and **8** [22,24] matched the previously reported spectra. For compound **4b**: ^{1}H NMR (250 MHz, $CDCl_3$): δ 9.02 (s, 2H), 4.30 (d, *J* = 8.7 Hz, 1H), 3.93 (m, 1H), 3.89 (sept, *J* = 6.6 Hz, 1H), 3.68 (m, 1H), 2.67 (m, 1H), 2.50 (q, *J* = 11.1 Hz, 2H), 2.26 (q, *J* = 12.3 Hz, 2H), 2.14 (d, *J* = 12.7 Hz, 2H), 1.94 (d, *J* = 7.0 Hz, 2H), 1.75-1.65 (m, 4H), 1.47 (d, *J* = 6.5 Hz, 6H), 1.33 (d, *J* = 7.6 Hz, 6H), 1.25-0.85 (m, 8H) ppm. ^{13}C NMR (360 MHz, $CDCl_3$): δ 154.6, 144.9, 131.1, 125.3, 120.3, 82.2, 67.4, 61.7, 51.6, 51.5, 31.5, 29.5,

28.8, 27.3, 26.6, 25.2, 23.8, 21.5 ppm. IR (KBr) ν = 3446, 2928, 2854, 1707, 1586, 1521, 1488, 1251, 1221, 1054 cm^{-1}. HRMS (ESI-QTOF) found m/z 584.2802; calculated for [M+Na]$^+$ 584.2803. For compound **5b**: ^{1}H NMR (250 MHz, CDCl$_3$) δ 9.02 (s, 2H), 4.53 (d, J = 7.5 Hz, 1H), 4.18 (sept, J = 7.5 Hz, 1H), 3.61 (m, 1H), 3.31 (quint, J = 7.5 Hz, 1H), 3.15 (sept, J = 7.5 Hz, 1H), 2.25 (m, 2H), 2.05-1.83 (m, 4H), 1.72 (d, J = 7.5 Hz, 6H), 1.50-1.28 (m, 8H), 1.23 (d, J = 7.6 Hz, 6H), 1.15-0.80 (m, 6H) ppm. ^{13}C NMR (400 MHz, CDCl$_3$): 154.7, 144.7, 131.0, 125.3, 120.2, 82.4, 62.1, 58.7, 58.2, 52.8, 34.1, 3145, 29.5, 27.1, 25.4, 25.3, 21.7, 19.5 ppm. IR (KBr) ν = 3416, 2936, 2857, 1711, 1586, 1524, 1487, 1431, 1313, 1204, 1185 cm^{-1}. HRMS (ESI-QTOF) found m/z 584.2804; calculated for [M+Na]$^+$ 584.2803.

2.2.2. Synthesis of compound **6b**

A solution of 2,6-dinitro-4-(trifluoromethyl)phenol (2.5 g, 9.9 mmol) in CH$_2$Cl$_2$ (35 mL) was slowly added to a solution of *N,N'*-dicyclohexylcarbodiimide (18.6 g, 95.0 mmol) in CH$_2$Cl$_2$ (20 mL). The reaction mixture was stirred at room temperature under argon atmosphere for 4 h. The organic solvent was removed under reduced pressure and the resulting solid redissolved in hot methanol (120 mL). Water (80 mL) was then added to this solution and stored at 0 °C for 72 h. A gelatinous mass was separated and purified by flash column chromatography (2:3 ethyl acetate:hexane), which yielded monosubstituted compound **9** (2.4 g, 65% yield) and target product **6b** (0.55 g, 11% yield). As already described for SZMC switch **2b** [20], compound **6b** was isolated as an irresoluble tautomeric mixture of **6b** and **6c** (6:96 and 15:85 molar ratios at 298 K and 238 K, respectively). At room temperature, only the NMR signals of major tautomer **6c** could be resolved. For **6b+6c**: ^{1}H NMR (400 MHz, CD$_3$CN, 298 K) 8.49 (s, 2H, **6c**), 4.17 (tt, J_1 = 5.0 Hz, J_2 = 10.3 Hz, 1H, **6c**), 3.47 (t, J = 10.4 Hz, 1H, **6c**), 3.20-3.10 (m, 2H, **6c**), 1.86-1.45 (m, 20H, **6c**), 1.43-0.94 (m, 20H, **6c**) ppm. ^{1}H NMR (400 MHz, CD$_3$CN, 238 K) 8.58 (s, 1H, **6c**), 8.48 (s, 1H, **6c**), 8.20 (s, 2H, **6b**), 4.80 (d, J = 9.2 Hz, 1H, **6b**), 4.24 (t, J = 10.7 Hz, 1H, **6c**), 3.69 (t, J = 11.8 Hz, 1H, **6b**), 3.55-3.26 (m, 2H, **6c**), 3.19 (t, J = 12.9 Hz, **6b**), 3.11-2.85 (m, 1H, **6b**, 1H, **6c**), 2.69 (tt, J_1 = 3.4 Hz, J_2 = 11.4 Hz, 1H, **6b**), 1.88-1.44 (m, 20H, **6b**, 20H, **6c**), 1.42-0.89 (m, 20H, **6b**, 20H, **6c**) ppm. ^{13}C NMR (100.6 MHz, CD$_3$CN, 298 K) 164.3 (**6c**), 157.9 (**6c**), 135.3 (**6c**), 130.8 (q, J = 37.6 Hz, **6c**), 128.6

(**6c**), 123.0 (q, J = 267.1 Hz, **6c**), 79.1 (**6c**), 64.7 (**6c**), 60.7 (**6c**), 56.2 (**6c**), 34.8 (**6c**), 32.8 (**6c**), 31.4 (**6c**), 29.3 (**6c**), 29.0 (**6c**), 25.5 (**6c**), 25.4 (**6c**), 25.3 (**6c**), 24.7 (**6c**) ppm. IR (KBr, 298 K) 2928, 2854, 1629, 1552, 1450, 1342, 1313, 1176, 1138, 897, 753, 718 cm^{-1}. HRMS (ESI-QTOF) found m/z 665.3632; calculated for $[M+H]^+$ 665.3638. **9**: ^{1}H NMR (360 MHz, CDCl$_3$) 8.28 (s, 2H), 4.26 (d, J = 7.4 Hz, 1H), 3.88 (tt, J = 12.1, 3.2 Hz, 1H), 3.71-3.58 (m, 1H), 1.99-1.86 (m, 2H), 1.86-1.51 (m, 8H), 1.44-1.21 (m, 4H), 1.21-0.88 (m, 6H) ppm. ^{13}C NMR (90.4 MHz, CDCl$_3$) 154.8, 151.0, 132.7, 131.6 (q, J = 36.3 Hz), 125.1 (q, J = 3.4 Hz), 121.6 (q, J = 273.9 Hz), 59.6, 50.1, 33.5, 32.1, 25.8, 25. 7, 25.3, 25.0 ppm. IR (KBr) 3308, 3093, 2934, 2858, 2051, 1629, 1534, 1450, 1380, 1344, 1312, 1256, 1179, 1130, 1063, 979, 914, 794, 754, 718, 698, 673 cm^{-1}. HRMS (ESI-QTOF) found m/z 459.1851; calculated for $[M+H]^+$ 459.1855.

2.2.3. Preparation of the potassium salts of **4a**, **5a** *and* **6a**

To prepare the anionic states of SZMC switches **4b**, **5b** and **6b**, the following general producedure was used. To a solution of the compound of interest (0.1 g) in acetonitrile, solid *t*BuOK was slowly added under argon atmosphere until the mixture was no longer fluorescent under UV (365 nm) light excitation. The red solution was filtered and the excess base removed. The organic solvent was evaporated under reduced pressure to afford the potassium salt of the anionic state with quantitative yield. Compound **4a**: ^{1}H NMR (400 MHz, CD$_3$CN) 8.77 (s, 2H), 3.68 (q, J = 7 Hz, 1H), 3.25-3.13 (m, 1H), 3.02 (sept, J = 6.9 Hz, 1H), 2.59-2.45 (m, 1H), 2.42-1.05 (m, 20H), 1.14 (d, J = 6.8 Hz, 6H), 1.10 (d, J = 6.1 Hz, 6H) ppm. Compound **5a**: ^{1}H NMR (400 MHz, CD$_3$CN) 8.69 (s, 2H), 3.65 (sept, J = 6.6 Hz, 1H), 3.47-3.36 (m, 1H), 3.03 (q, J = 6.8 Hz, 1H), 2.70-2.50 (m, 1H), 1.75-1.11 (m, 20H), 1.51 (d, J = 6.7 Hz, 6H), 1.07 (d, J = 6.7 Hz, 6H) ppm. Compound **6a**: ^{1}H NMR (250 MHz, CD$_3$CN, 298 K) 8.05 (s, 2H), 3.30 (m, 2H), 3.15 (m, 2H), 1.80-0.88 (m, 40H) ppm.

3. RESULTS AND DISCUSSION

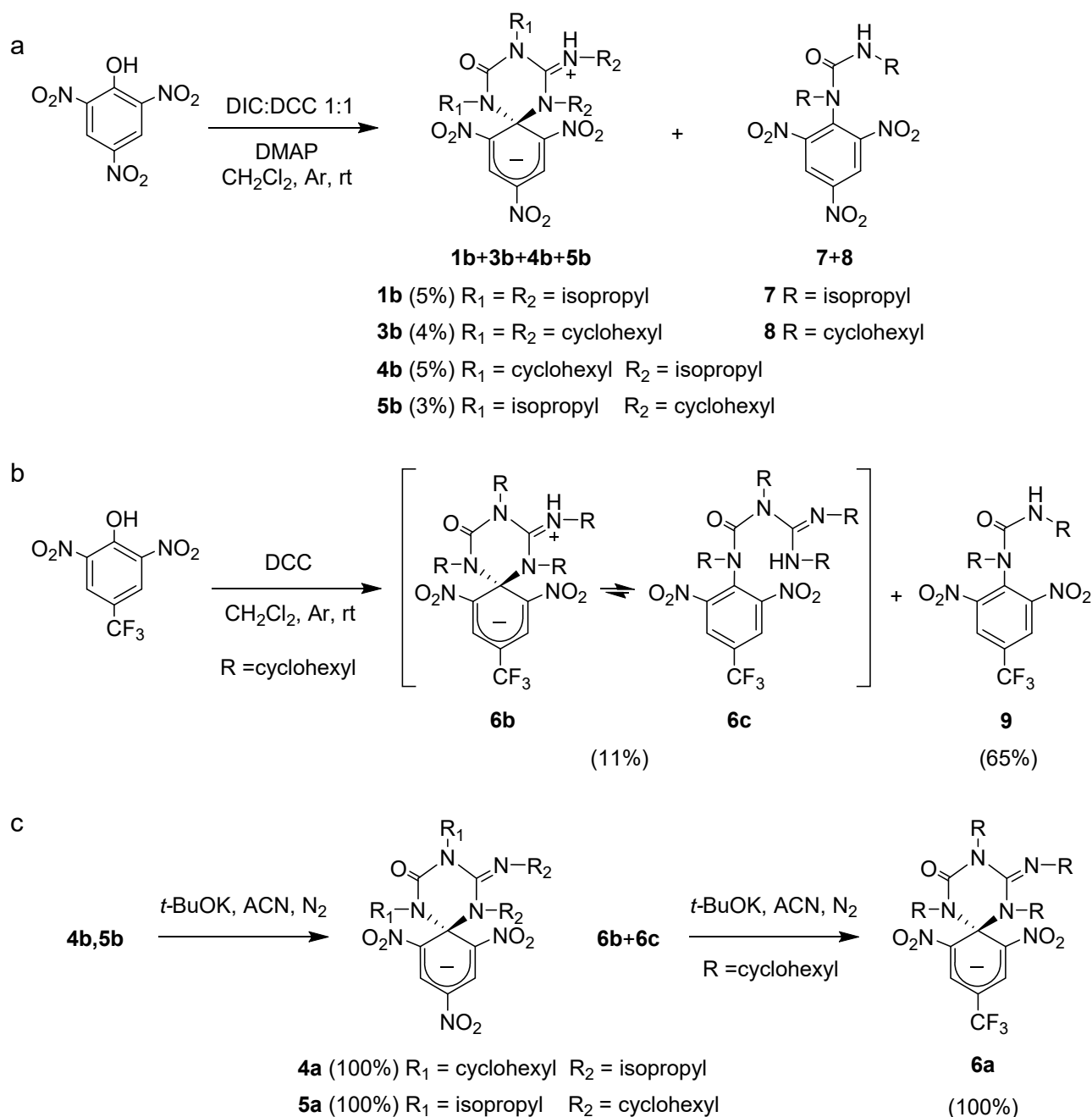## 3.1. Synthesis of new SZMC switches

More than a decade has passed since we first reported the synthesis of SZMC **1b** [12] featuring molecular switching behavior by direct reaction of *N*,*N*$^{'}$-diisopropylcarbodiimide (DIC) with picric acid. Analogues

of this compound were subsequently prepared by applying this procedure to other commercially available phenols (2,6-dinitro-4-(trifluoromethyl)phenol) and carbodiimides (*N,N'*-dicyclohexylcarbodiimide, DCC), thus obtaining fluorescent switches **2b** [20] and **3b** [22,24]. In an attempt to expand this family of functional molecules, we explored the preparation of new SZMC compounds using the same one-pot synthetic methodology.

Firstly, we assay the reaction between DIC and other electron-poor aromatic phenols, such as 2,4-dinitrophenol, 4-nitrophenol and nitrated naphthols, none of which provided a spirocyclic adduct similar to SZMC. From this we inferred that the formation of SZMCs requires the parent aromatic system to bear sufficient strong electron-withdrawing groups as to stabilize the cyclohexadienyl anion, mainly through resonance effects. For this reason, we decided to preserve the 2,4,6-trisubstitution pattern of the cyclohexadienyl anions of **1b-3b**, and focused our efforts on varying the nature of the reacting carbodiimide (i.e. of the substituents of the triazene ring of the final compound). In particular, we prepared two different types of novel SZMC switches composed of: (a) a 2,4,6-trinitrocyclohexadienyl anion and a triazene group with mixed isopropyl and cyclohexyl chains (**4b** and **5b**); (b) a 2,6-dinitro-4-(trifluoromethyl)cyclohexadienyl anion and a cyclohexyl-decorated triazene ring (**6b**).

For the synthesis of compounds **4b** and **5b** we took advantage of the fact that the addition of the two carbodiimide groups to the phenol derivative is not concerted, but instead proceeds sequentially (Scheme S1) [13]. As such, the reaction of picric acid with equimolar amounts of DIC and DCC should furnish a statistical mixture of four different SZMCs (**1b**, **3b**, **4b** and **5b**, Scheme 2a). Spectroscopic analysis of the fractions obtained after purification of the reaction crude indeed revealed the formation of all these products in similar yields. Monosubstitution products **7** and **8** were also obtained, as previously described for the synthesis of **1b-3b** [12,13,22,24], which further confirms the stepwise nature of the reaction mechanism. Structural elucidation of compounds **4b** and **5b** was accomplished by means of ^{1}H NMR COSY (Fig. S2). For compound **4b**, cross-peaks were found in the COSY spectrum between the guanidinium NH proton (δ 4.30 ppm) and an isopropyl CH proton (δ 3.93 ppm), while cross-correlation

was observed between the guanidinium NH proton (δ 4.53 ppm) and a cyclohexyl CH proton (δ 3.61 ppm) in the case of **5b**.

Scheme 2. (a-b) Synthesis of SZMC switches **4b**, **5b** and **6b**. (c) Preparation of the anionic states of these switches. DIC: *N,N'*-diisopropylcarbodiimide; DCC: *N,N'*-dicyclohexylcarbodiimide; DMAP: 4-dimethylaminopyridine.

Compound **6b** was prepared by direct reaction between 2,6-dinitro-4-(trifluoromethyl)phenol and excess DCC (Scheme 2b). As expected, both the target product and the monosubstituted derivative **9** were formed in this process. More interestingly, **6b** was isolated as an irresoluble mixture of two different interconverting tautomers: the spirocyclic zwitterionic complex **6b** and the neutral aromatic compound **6c**. This behavior has already been reported for the analogous compound **2b** (Scheme 1a) and was attributed to a lower stabilization of the cyclohexadienyl anion of the SZMC product via resonance effects when replacing one nitro substituent by a trifluoromethyl group [20]. ^{1}H NMR analysis revealed that the composition of **6b** and **6c** equilibrium mixture is temperature dependent with the stability of **6b** decreasing with increasing temperature (see Section 3.2.5 for additional discussion). Thus, the ratio of **6b:6c** diminishes from 15:85 to 5:95 upon raising the temperature of the solution from 238 K to 298 K. It is worth noting that a larger population of the zwitterionic tautomer was measured for SZMC switch **2**, the molar ratio for the **2b-2c** equilibrium mixture in acetonitrile at room temperature being 23:77. This difference might be attributed to the larger steric hindrance imparted by the cyclohexyl groups, which should further destabilize the spirocyclic structure of **6b**. Therefore, this appears to be an additional factor to consider when designing new SZMC switches, aside from the nature and number of electron-withdrawing substituents in the initial aromatic phenol.

To confirm that the steric effects caused by the pendant groups attached to the starting carbodiimides play a pivotal role in the formation of a stable spyrocyclic Meisenheimer compounds, additional experiments were conducted. Firstly, we attempted the reaction between picric acid and commercially available carbodiimides bearing bulkier side groups: *N,N'*-di-*tert*-butylcarbodiimide and *N,N'*-bis(trimethylsilyl)carbodiimide. None of these carbodiimides were able to form stable SZMC compounds. Secondly, we investigated the thermal stability of **1b** and **3b** by means of ^{1}H NMR. For both compounds, broadening of their narrow NMR proton signals was observed upon substantial heating, which was ascribed to destabilization of their spirocyclic structures and reversible transformation into the corresponding aromatic tautomers analogous to **2c** and **6c** (Fig. S3). Since such interconversion process occurred at high temperatures and, as such, at high rates, it could not be resolved by ^{1}H NMR, thus

yielding broad resonances in the spectrum instead of two separate sets of signals. Interestingly, the onset of this dynamic behavior was observed at a higher temperature for **1b** (T ~ 398 K) than **3b** (T ~ 353 K), which suggests that the spirocyclic structure of the former is further stabilized due to the lower steric hindrance imparted by the isopropyl groups when compared to cyclohexyl substituents.

With compounds **4b**, **5b** and **6b-6c** at our disposal, we finally assayed the formation of their anionic states **4a**, **5a** and **6a** by adding the appropriate amount of base (Scheme 2c). For all these compounds, deprotonation of the starting material took place quantitatively and, in the case of the **6b-6c** mixture, transformation of both tautomers into a single anionic spirocyclic complex was observed. This is a further proof that **6b** and **6c** are isomeric species which continuously interconvert in solution.

3.2. Characterization of new SZMC switches

3.2.1. Optical properties of 4, 5 and 6

Fig. 1a shows the absorption spectra measured for the neutral and anionic states of **4** and **5** in acetonitrile. In both cases strong absorption of visible light and noticeable spectral changes upon interconversion between their anionic and zwitterionic states were observed. In particular, two different absorption bands were registered in the visible region corresponding to the $S_0 \rightarrow S_1$ and $S_0 \rightarrow S_2$ electronic transitions of these compounds, the maxima of which were found at 524 and 432 nm for **4a** and **5a** and at 528 and 408 nm for **4b** and **5b** in acetonitrile (Table 1). Although no spectral differences were observed between these two SZMC switches, slightly larger molar extinction coefficients (ε) were measured for **5b** (Table 1), which uncovers a non negligible effect of the R group susbstituent of the triazene ring on the absorption properties of the nearby cyclohexadienyl anion. In view of this result and the data reported for **1b** and **3b**, we concluded that surrounding the guanidinium/guanidine group of SZMC with cyclohexyl substituents generally increases its ε values (Table 1).
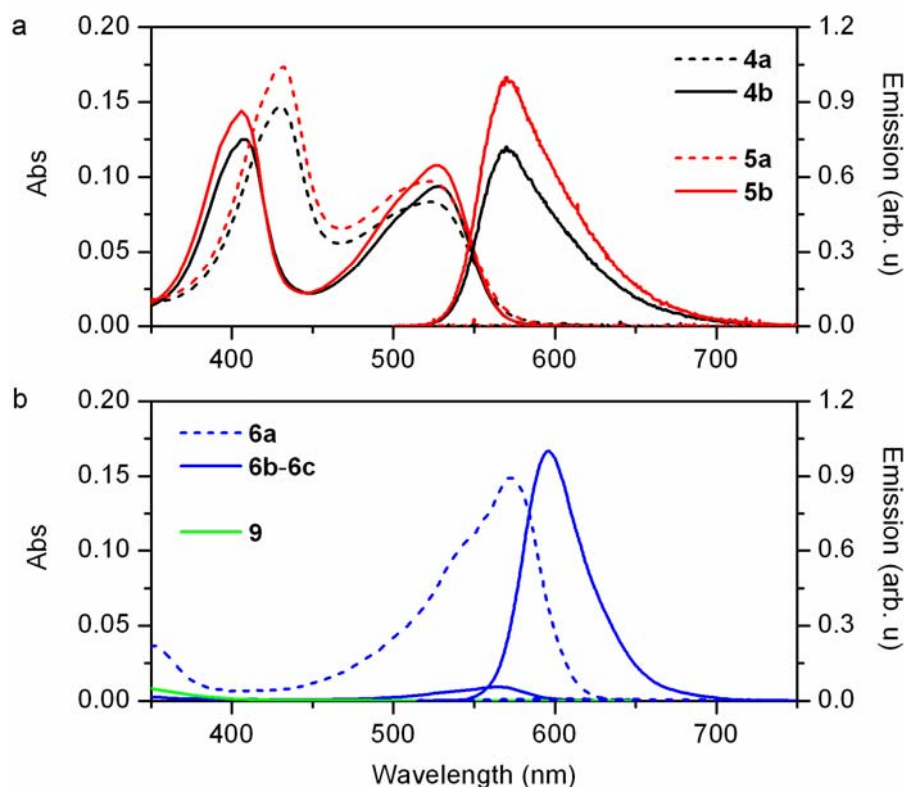
Fig. 1. Absorption and fluorescence spectra of (a) **4a**, **4b**, **5a** and **5b**, and (b) **6a**, **6b-6c** and **9** in acetonitrile at 298 K (c = 1.0x10^{-5} M, λ_{exc}= 473 nm for **4** and **5**, λ_{exc}= 532 nm for **6** and **9**).

Table 1. Optical properties of **4-6** and previously reported SZMC switches **1-3** in acetonitrile at 298 K.

	$\lambda_{abs,max}$ (nm) [ε (M^{-1} cm^{-1})]		$\lambda_{abs,max}$ (nm) [ε (M^{-1} cm^{-1})]	$\lambda_{fl,max}$ (nm) [Φ_{fl}]
1a [a]	432 [15299], 524 [9059]	**1b** [a]	408 [12840], 528 [11253]	569 [0.50]
3a [b]	432 [18585], 524 [11031]	**3b** [b]	408 [16664], 528 [11191]	569 [0.67]
4a	432 [14732], 524 [8321]	**4b**	408 [12232], 528 [9368]	570 [0.52]
5a	432 [17444], 524 [9655]	**5b**	408 [14807], 528 [10771]	570 [0.64]
2a [c]	576 [14123]	**2b-2c** [c]	564 [14913 [d]]	594 [0.76 [d]]
6a	573 [14534]	**6b-6c**	565 [15383 [d]]	594 [0.78 [d]]

[a] Ref. [15]. [b] Measured in this work. [c] Ref. [20]. [d] Intrinsic ε and Φ_{fl} values of **2b** and **6b**, since only these isomers absorb and emit in the visible region.

The anionic and zwitterionic states of **4** and **5** also clearly differed in their fluorescent properties (Fig. 1a). Whereas nearly no fluorescence emission was registered for **4a** and **5a**, a large increase in emission intensity was observed for **4b** and **5b** ($\lambda_{fl,max}$ = 570 nm). Based on the behavior described for previous SZMC switches [15,20], fluorescence quenching in the anionic state of **4** and **5** must be ascribed to photoinduced electron transfer (PET) from the deprotonated guanidine group in the triazene ring towards the 2,4,6-trinitrocyclohexadienyl anion. Upon protonation of the guanidine group, this emission quenching mechanism is inhibited and the zwitterionic states of **4** and **5** recover the strong fluorescence of their cyclohexadienyl chromophore. It must be noted that the emission quantum yield (Φ_{fl}) of such state varies with the nature of the R group on the triazene ring and, especially, of those attached to the guanidinium moiety. Thus, a 23% increase in Φ_{fl} was observed between **4b** and **5b** ($\Phi_{fl,4b}$= 0.52 and $\Phi_{fl,5b}$= 0.64), in agreement with what was registered for **1b** and **3b** only bearing isopropyl and cyclohexyl substituents, respectively (Table 1). Most likely, this indicates that the presence of bulky groups around the guanidinium moiety lowers the probability of the intrinsic non radiative relaxation pathways of the adjacent 2,4,6-trinitrocyclohexadienyl anion chromophore, thereby increasing the fluorescence quantum yield.

Replacement of one nitro group by a CF$_3$ group in the cyclohexadienyl anion of SZMC switches is known to decrease the excitation energy of this chromophore [20]. This behavior was indeed observed for new compound **6** in acetonitrile, which shows a red-shifted absorption band at *ca.* 570 nm for both **6a** and the equilibrium mixture of **6b** and **6c** (Fig. 1b and Table 1). However, the absorption intensities registered for the two states of **6** were dramatically different, the intensity of the band measured for **6a** being about 20-fold larger. This is due to the different optical properties of the coexisting **6b** and **6c** tautomers. While the former has the same 2,6-dinitro-4-(trifluoromethyl)cyclohexadienyl anion chromophore as **6a**, the latter presents an aromatic 2,6-dinitro-4-(trifluoromethyl)phenyl group with a completely different behavior. In particular, **6c** is not expected to absorb visible light, by analogy with compound **9** bearing the same chromophore unit (Fig. 1b). Therefore, only the small amount of spirocyclic zwitterionic molecules in the

6b-6c equilibrium mixture (5% in acetonitrile at 298 K) are responsible of the absorption band at 565 nm, thus justifying the lower intensity measured with respect to **6a**. Actually, when accounting for this situation, the ε value determined for **6b** is very similar to that of the anionic state of the switch (Table 1). In spite of the lack of optical activity in the visible region of the major tautomer **6c**, intense emission was measured for the **6b-6c** equilibrium mixture in acetonitrile at room temperature ($\lambda_{fl,max}$ = 594 nm), which strikingly diminished upon transformation into **6a** (Fig. 1b). As previously discussed for **4a** and **5a**, this is due to the very low fluorescence quantum yield of **6a**, which results from a PET-based quenching mechanism of its chromophore emission when the guanidine unit is deprotonated. On the contrary, a large Φ_{fl} value was determined for **6b** upon protonation of the guanidine group (Φ_{fl} = 0.78), which is slightly higher than that previously reported for **2b** (Table 1). This, together with the larger ε values also measured for **6**, further confirms that the optical properties of SZMC switches improve when replacing the isopropyl groups of the triazene ring by cyclochexyl substituents.

3.2.2. Electrochemical properties of **4**, **5** and **6**

Fig. 2a shows the cyclic voltammograms of the anionic and spirocyclic states of **4** and **5** in acetonitrile, which resemble those measured for **1** [19] and **3** (Fig. S4). When starting from a cathodic scan, two successive one-electron reversible waves were registered at *ca*. -1.2 V and -1.5 V (vs SCE) for **4a** and **5a**, which indicate the formation of the stable dianion and trianion of these species, respectively. In the subsequent anodic scan, two one-electron waves were found, an irreversible wave at *ca*. +1.0 V (vs SCE) followed by a reversible wave at *ca*. +1.5 V (vs SCE) (Table 2). Interestingly, the latter was also encountered in the cyclic voltammograms of **4b** and **5b** when starting form an anodic scan, which suggests that it corresponds to the generation of the corresponding radical cation of these zwitterionic compounds. In their cathodic scan a one-electron irreversible wave was first observed at *ca*. -0.8 V (vs SCE) and, subsequently, two additional reversible reduction waves were registered at *ca.* -1.2 V and -1.5 V (vs SCE), which matched those also registered for **4a** and **5a** (Table 2).
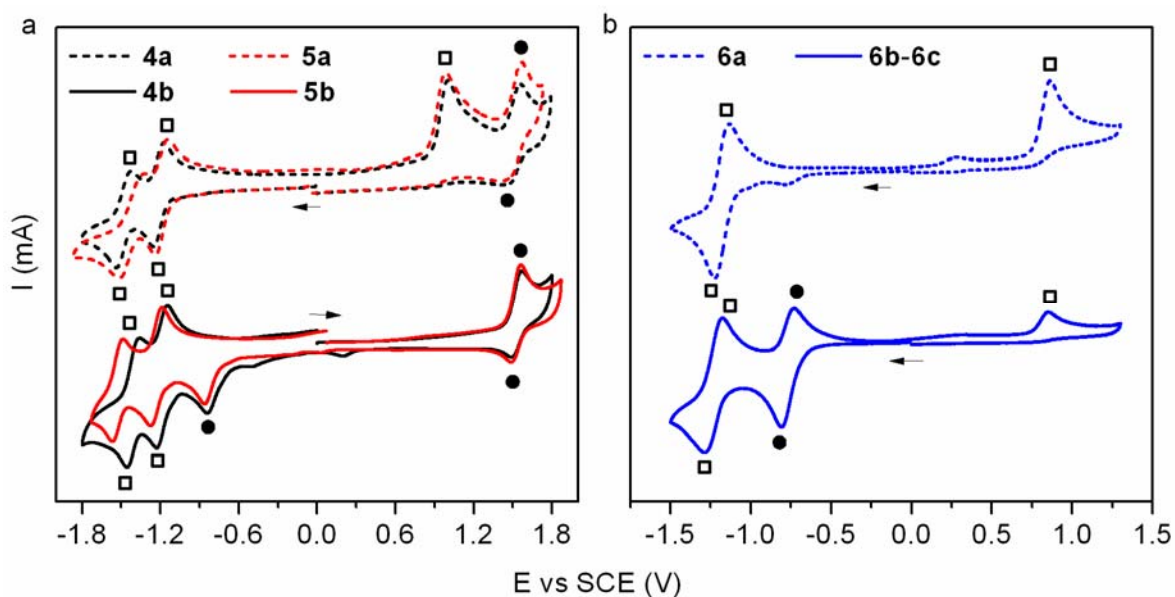
Fig. 2. Cyclic voltammograms of (a) **4a**, **4b**, **5a** and **5b**, and (b) **6a** and **6b-6c** in acetonitrile at 298 K (c = 5.0x10^{-4} M, 0.1 M n-Bu$_4$NPF$_6$, scan rate = 0.5 V s^{-1}). Solid circles and hollow squares are used to assign the electrochemical waves arising from the anionic (•) and neutral states (□) of these compounds, respectively. Arrows indicate the direction of the potential scan in each case.

The measurement of equivalent redox waves in the cyclic voltammograms of the anionic and zwitterionic states of SZMCs is ascribed to electrochemically-induced interconversion between those species. In particular, the irreversible oxidation process at *ca.* +1.0 V (vs SCE) should induce guanidine protonation of **4a** and **5a** by sequential neutral radical formation and hydrogen atom abstraction from the solvent, thus leading *in situ* to **4b** and **5b**. As such, this would account for the reversible wave of the zwitterionic states of **4** and **5** at *ca.* +1.5 V (vs SCE) measured in the cyclic voltammograms of their anionic counterparts. In a similar fashion, reduction of **4b** and **5b** at *ca.* -0.8 V (vs SCE) should result in guanidinium deprotonation and transformation into **4a** and **5a**, the reversible reduction waves of which at *ca.* -1.2 V and -1.5 V (vs SCE) then appearing in the cyclic voltammogram of the zwitterionic compounds. Deeper analysis of this redox-induced process revealed that it proceeds via anion radical formation of **4b** and **5b** followed by hydrogen atom elimination with a rate constant of 390 s^{-1}.

Table 2. Electrochemical properties of **4-6** and previously reported SZMC switches **1-3** in acetonitrile.[a]

	E_{ox} (V) [b]	E_{red} (V) [c]		E_{ox} (V) [c]	E_{red} (V) [d]
1a [e]	+0.98	-1.20, -1.48	**1b** [e]	+1.52	-0.85
3a [f]	+0.98	-1.20, -1.48	**3b** [f]	+1.53	-0.82
4a	+0.98	-1.20, -1.46	**4b**	+1.51	-0.86
5a	+0.95	-1.18, -1.45	**5b**	+1.51	-0.86
2a [g]	+0.89	-1.14	**2b-2c** [g]	+1.37	-0.78
6a	+0.86	-1.18	**6b-6c**	+1.45[h]	-0.80

[a] All the potentials given are referred to saturated calomel electrode (SCE). Measurements in 0.1 M *n*-Bu4NPF6, scan rate 0.5 V s^{-1} and room temperature. [b] Irreversible wave; anodic peak potential is given. [c] Reversible waves; E^0 is given. [d] Irreversible wave; cathodic peak potential is given. [e] Ref. [15]. [f] Measured in this work. [g] Ref. [20]. [h] Determined when opening the electrochemical window up to +2 V (vs SCE).

Compound **6** displayed a similar redox behavior (Fig. 2b, Table 2). In the case of the anionic state **6a**, two main waves were detected by cyclic voltammetry: (a) a one-electron reversible reduction wave at -1.18 V (vs SCE) attributed to the formation of the dianion of this compound; (b) a one-electron irreversible oxidation wave at +0.86 V (vs SCE), which is expected to induce transformation into **6b-6c** by guanidine group protonation via neutral radical formation and hydrogen atom abstraction from the solvent. Interestingly, these two redox waves were also observed in the cyclic voltammogram of **6b-6c**, together with an additional pseudo-reversible reduction wave at -0.80 V (vs SCE). Accordingly, the latter must lead to the formation of the unstable radical anion of **6b**, which should slowly undergo hydrogen atom elimination to generate **6a** and, as such, give rise to the redox waves of this compound. Because of the equilibrium process found in solution between **6b** and **6c**, this should therefore allow reversible electrochemical interconversion between the neutral and anionic states of the switch.

3.2.3. Molecular switching behavior of 4 and 5 using chemical stimuli

In view of the acid-base activity of the guanidine moiety of **4** and **5**, we first explored reversible switching operation of these compounds upon pH variation. Controlled amounts of acid ($HClO_4$) and base (tetrabutylammonium hydroxide, TBAOH) were added to acetonitrile solutions of **4a-5a** and **4b-5b**, respectively, and the guanidine protonation-deprotonation process was monitored by UV-vis absorption spectroscopy, cyclic voltammetry and fluorescence spectroscopy. In all the cases, we collected clear spectroscopic and electrochemical evidences of reversible and quantitative interconversion between the anionic and zwitterionic states of **4** and **5**after titration with 1 equivalent of acid and base.

On the one hand, spectral changes in the absorption spectra were registered that are indicative of the transformation between **4a-5a** (with bands at 432 and 524 nm) and **4b-5b** (with bands at 408 and 528 nm) (Fig. 3a and Fig. S5a). Noticeably, defined isosbestic points were observed in the spectra upon acid-base titration, thus ruling out the occurrence of pH-induced degradation of these compounds. In addition, acid-base switching was corroborated by the variation of the peak currents of the irreversible redox waves that are characteristic of the zwitterionic (reduction wave at *ca.* -0.8 V (vs SCE)) and anionic states (oxidation wave at *ca.* +1.0 V (vs SCE)) of **4** and **5** (Fig. 3b and Fig. S5b). Finally, *on-off* modulation of the fluorescence emission was also achieved by acid-base addition, as expected due to the non emissive behavior of **4a** and **5a** (Fig. 3c and Fig. S5c). All these experiments unambiguously demonstrated that **4** and **5** are pH-sensitive molecular switches, the operation of which was shown to be robust and reversible at least for 6 cycles of acid-base addition (Fig. 4).
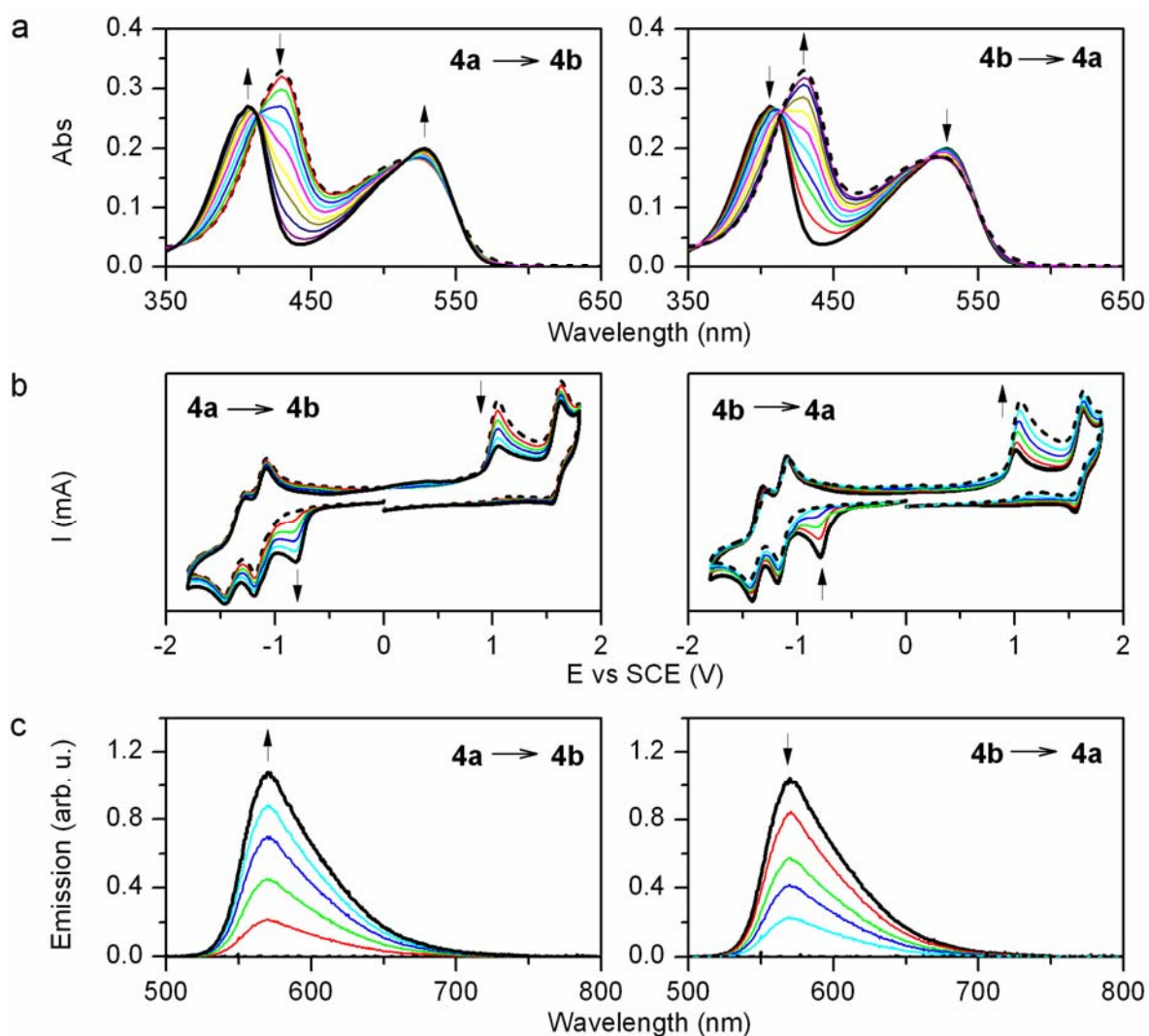
Fig. 3. Acid-base interconversion between **4a** and **4b** monitored by (a) UV-vis absorption spectroscopy (c = 2.2x10^{-5} M, acetonitrile, 298 K), (b) cyclic voltammetry (c = 2.2x10^{-3} M, acetonitrile + 0.1 M n-Bu$_4$NPF$_6$, scan rate 0.5 V s^{-1}, 298 K), and (c) fluorescence spectroscopy (c = 1.5x10^{-5} M, acetonitrile, λ_{exc}= 473 nm, 298 K). In each case increasing amounts of HClO$_4$ or TBAOH were added until reaching *ca*. 1 equivalent of acid or base.
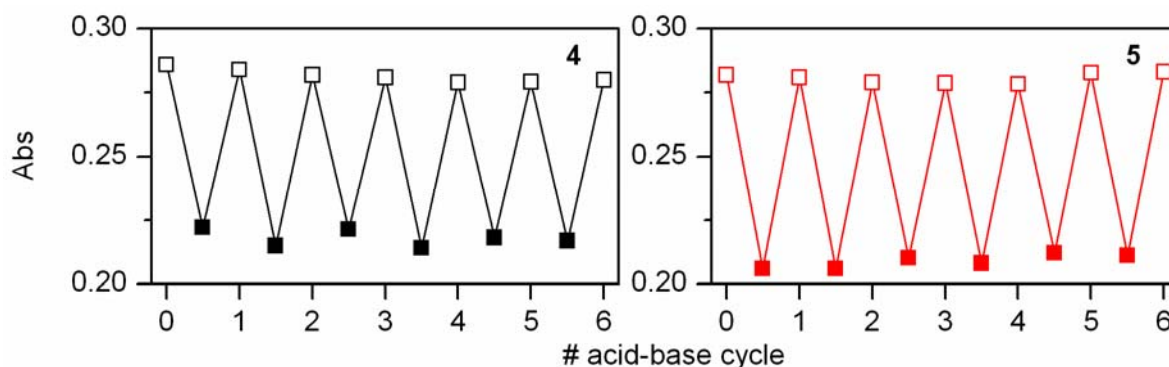
Fig. 4. Variation of the absorbance at 406 nm during 6 consecutive cycles of acid-base switching of **4** and **5**. The absorbance of the zwitterionic states of these compounds is shown in solid symbols, while hollow symbols are used for their anionic forms.

This halochromic response can be applied for selective detection of Brönsted bases such as fluoride and cyanide anions, which can deprotonate the guanidinium group of **4b** and **5b** and, consequently, lead to quenching of their fluorescence emission. In the case of fluoride ion detection, similar results were obtained for **4b** and **5b** to those already reported for compounds **1b** and **3b** [22,23]. In particular, selective fluorescence "turn off" was observed when 1.2 equivalents of fluoride were added to ACN or THF solutions of either **4b** or **5b**, whereas no significant changes were found for other halide ions (Figure 5a). As such, these compounds could also be used as fluorescent fluoride chemosensors. By contrast, the response to cyanide ions was found to strongly depend on the solvent and the nature of the pending chains in the triazene ring of SZMC switches. On the one hand, acetonitrile solutions of **1b**, **3b**, **4b** and **5b** showed analogous behavior and, in all the cases, complete emission quenching was measured upon addition of 1.2 equivalents of CN⁻ anions (Figure 5b). When using TFH as a solvent, however, different results were obtained for these compounds (Figure 5c): while nearly complete fluorescence "turn off" was observed for **1b** after adding 1.2 equivalents of CN⁻ anions, minor changes were registered for SZMC switches bearing cyclohexyl groups and, indeed, nearly no effect in emission was measured for **3b**. Actually, the fluorescence response to cyanide ions (ΔF_{CN^-}) was found to gradually vary with the number of cyclohexyl groups introduced in the triazene ring ($\Delta F_{CN^-,1b} > \Delta F_{CN^-,4b}$, $\Delta F_{CN^-,5b} > \Delta F_{CN^-,3b}$) and their proximity to the pH-sensitive guanidium moiety ($\Delta F_{CN^-,4b} > \Delta F_{CN^-,5b}$), a behavior that was also observed colorimetrically

21

(Figure 5d). This demonstrates that variation of the substituents around this group modulates its acidity and, consequently, its sensitivity towards chemical analytes such as Brönsted bases. In our case, this allowed tailoring the optical chemosensing capacity of SZMC switches to cyanide ions in THF solution by simply replacing isopropyl with cyclohexyl groups in their triazene ring.
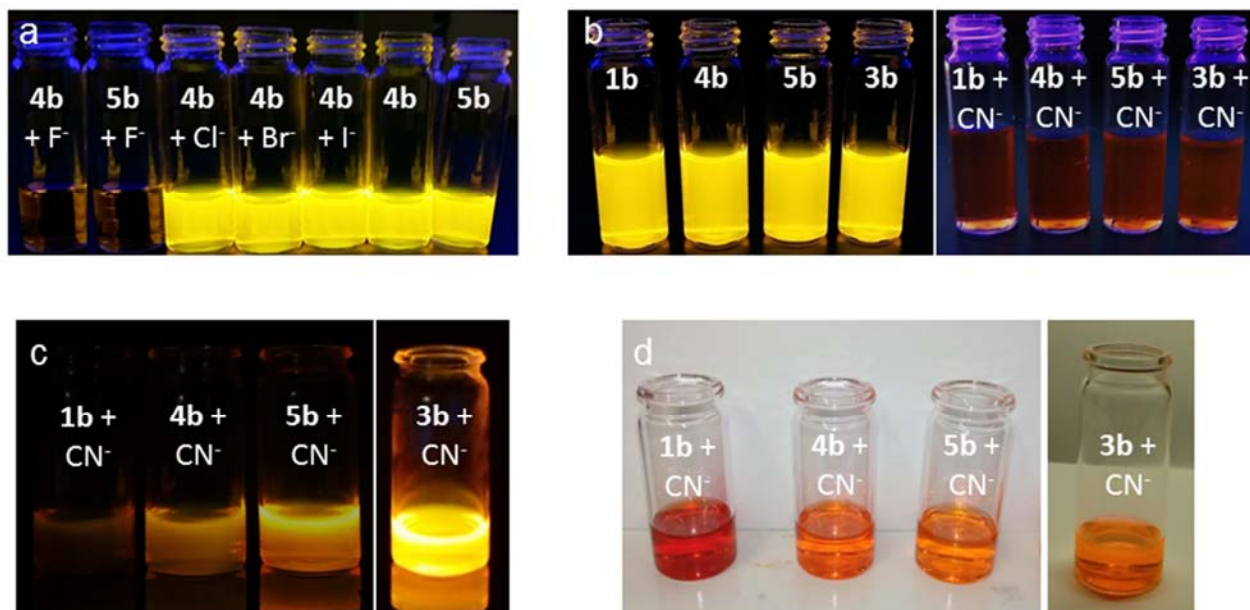

Fig. 5. (a) Fluorescence response of **4b** and **5b** (1 mM) in acetonitrile solution upon addition of 1.2 equivalents of fluoride, chloride, bromide, and iodide anions. (b) Fluorescence response of **1b**, **3b**, **4b** and **5b** (1 mM) in acetonitrile solution upon addition of 1.2 equivalents of cyanide anions. (c-d) Fluorescence and colorimetric response of **1b**, **3b**, **4b** and **5b** (1 mM) in THF solution upon addition of 1.2 equivalents of cyanide anions.

3.2.4. Molecular switching behavior of **4** and **5** using electrochemical stimuli

One of the main advantages of SZMC switches is that they can be operated by means of redox stimuli [15,19,20,22]. This, together with the electrochemical properties established for **4** and **5**, prompted us to investigate the switching between their anionic and spirocyclic states by means of reduction and oxidation processes. In addition, this study was expanded to analogous compound **3**, since only the acid-base operation of this switch had been previously reported [24]. With this aim, we first conducted controlled
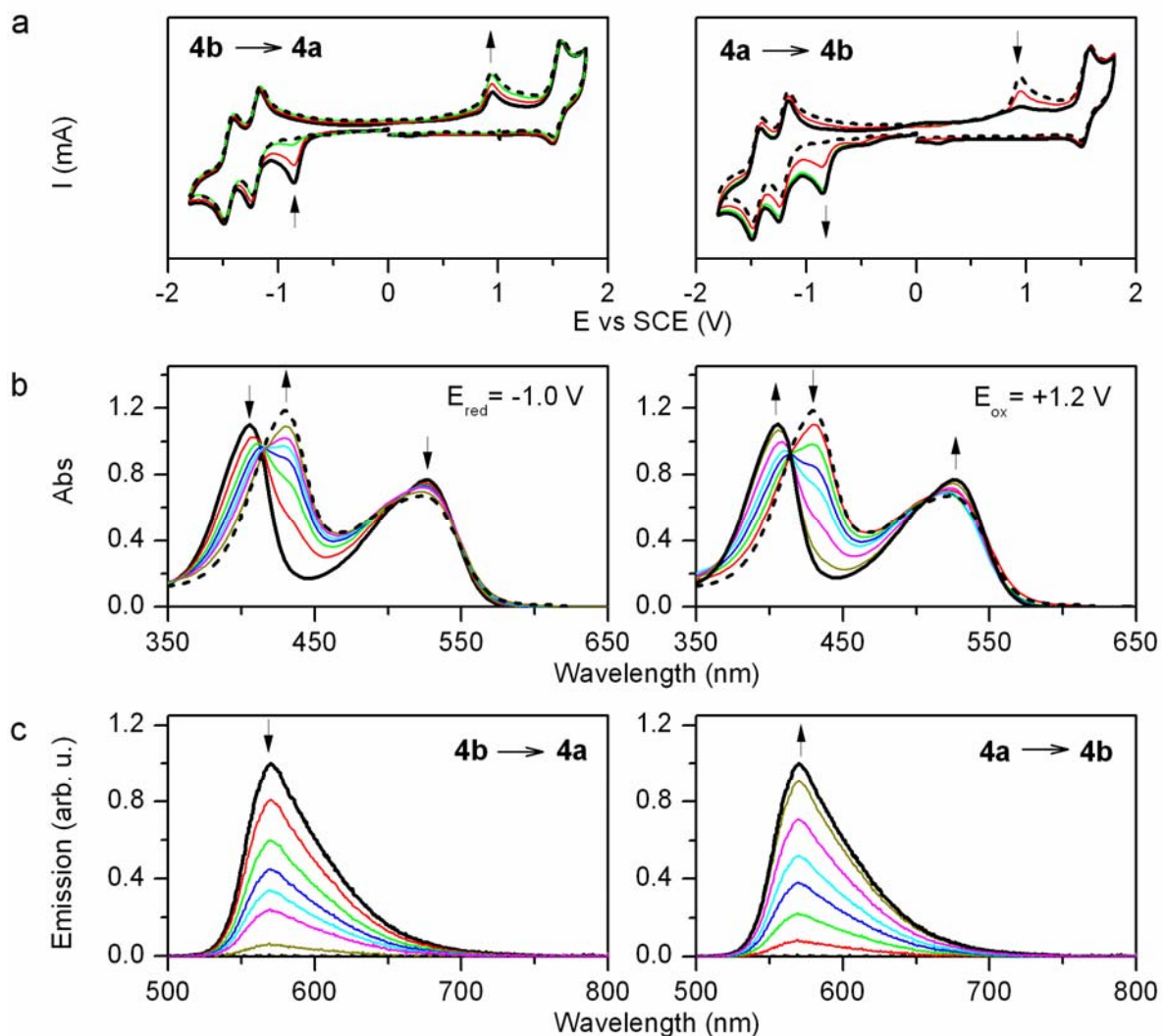
Fig. 6. Redox interconversion between **4a** and **4b** monitored by (a) cyclic voltammetry (c = 2.2x10^{-3} M, acetonitrile + 0.1 M n-Bu$_4$NPF$_6$, scan rate 0.5 V s^{-1}, 298 K), (b) UV-vis absorption spectroscopy (c = 8.0x10^{-5} M, acetonitrile, 298 K), and (c) fluorescence spectroscopy (c = 1.5x10^{-5} M, acetonitrile, λ_{exc}= 473 nm, 298 K). In each case increasing amounts of current were injected until reaching *ca.* 1.25 F for both the reductive (-1.0 V (vs SCE) for **4b** → **4a** conversion) and oxidative (+1.2 V (vs SCE) for **4a** → **4b** conversion) electrolysis conducted.

potential electrolysis of **3b-5b** at -1.0 V (vs SCE), a more negative potential than that of the irreversible reduction wave that these products present. Analysis of the electrolysed solution by cyclic voltammetry showed the disappearance of the reduction peak of these zwitterionic species at *ca.* -0.8 V (vs SCE) and

the appearance of the oxidation peak of their anionic derivatives at *ca.* +1.0 V (vs SCE) (Fig. 6a, Fig. S6a and Fig. S7a). Actually, after the passage of 1.25 F, we could corroborate by ^{1}H NMR that **3b-5b** were fully converted into **3a-5a**. The electrochemical reversibility of this process was then demonstrated by applying controlled potential electrolysis at +1.2 V of the previously obtained solutions of the anionic states of **3-5**, at which the unstable neutral radical of both species was generated that should evolve into their zwitterionic forms. Cyclic voltammetry of the resulting samples revealed the quantitative conversion of **3a-5a** into **3b-5b** (Fig. 6a, Fig. S6b and Fig. S7b), as also shown by ^{1}H-NMR.

The electrochemical-driven switching of **3-5** could also be established spectroscopically by means of absorption and emission measurements. On the one hand, we conducted spectroelectrochemical experiments where the variations in the UV–vis absorption spectra of these species could be monitored *in situ* during an electrolytical process (Fig. 6b, Fig. S6c-d and Fig. S7c-d). Clearly, when applying a combined sequence of reductive and oxidative electrolysis to acetonitrile solutions of **3b-5b**, changes in absorption were observed that are indicative of reversible transformation of these compounds into their anionic derivatives. Moreover, emission spectra measurements taken at selected electrolysis times were also compatible with these results (Fig. 6c), which allowed us concluding that compounds **3-5** also behave as redox-responsive fluorescent switches.

3.2.5. *Molecular switching behavior of* **6**

Acid-base and redox fluorescence switching of compound **6** was also investigated using spectroscopic and electrochemical techniques. As shown in Fig. 7, sequential addition of 1 equivalent of base (TBAOH) and 1 equivalent of acid (HClO4) allowed reversible interconversion between **6a** and **6b-6c**. On the one hand, this was demonstrated by monitoring the peak currents of the oxidation wave at +0.86 V (vs SCE) and the reduction wave at -0.77 V (vs SCE), which are characteristic of **6a** and **6b-6c**, respectively (Fig. 7a). On the other hand, the *on-off* fluorescence modulation measured upon pH-variation further confirmed transformation between the anionic and neutral states of the switch (Fig. 7b).
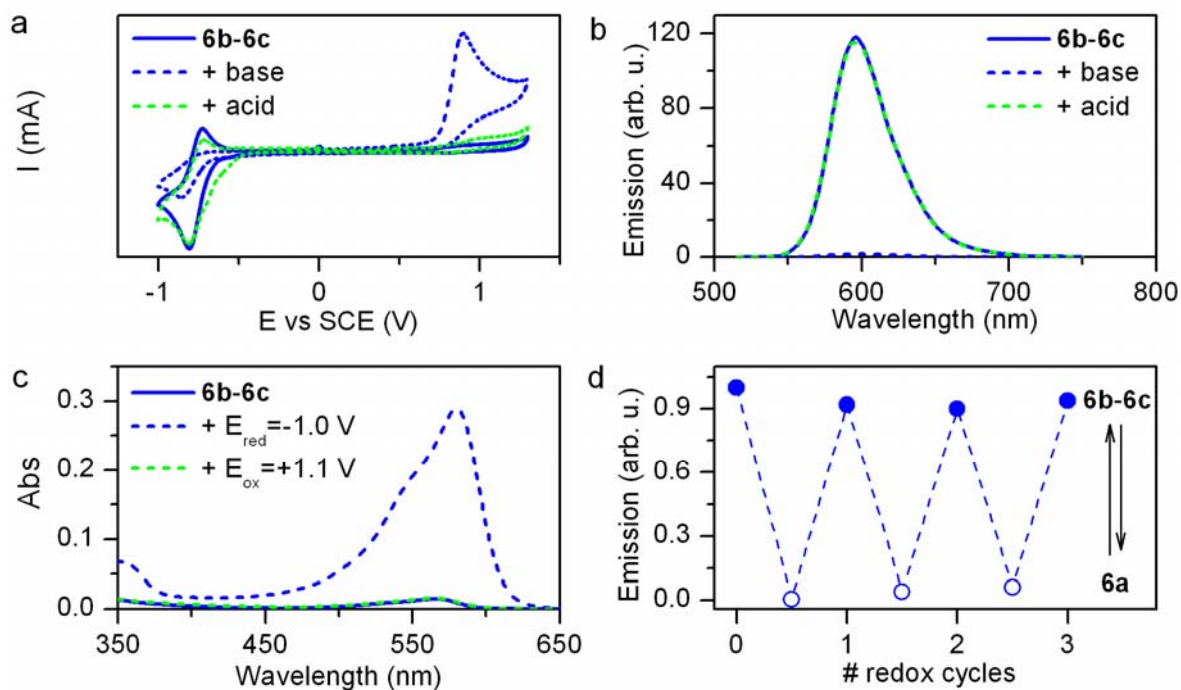
Fig. 7. (a-b) Variation of (a) the cyclic voltammogram (0.1 M *n*-Bu$_4$NPF$_6$, scan rate 0.5 V s^{-1}) and (b) the emission spectrum (λ_{exc}= 532 nm) of an acetonitrile solution of **6b-6c** at 298 K upon sequential addition of 1 equivalent of TBAOH and 1 equivalent of HClO$_4$. (c) Variation of the UV-vis absorption spectrum of an acetonitrile solution of **6b-6c** at 298 K upon sequential reductive and oxidative electrolysis at -1.0 V and +1.1 V (vs SCE), respectively. (d) Variation of the emission intensity of an acetonitrile solution of **6b-6c** at 298 K when subjected at 3 cycles of sequential reductive and oxidative electrolysis at -1.0 V and +1.1 V (vs SCE), respectively.

Similar results were achieved by applying sequential reductive and oxidative electrolysis at +1.1 V and -1.0 V (vs SCE) to induce protonation and deprotonation of the guanidine group of **6**, respectively. In this case, the occurrence of redox-induced switching was revealed by the changes observed in the absorption and emission spectra of the system (Fig. 7c-d), which arose from the different optical properties of **6a** and **6b-6c** already discussed. Importantly, this interconversion process was found to be fully reversible and repetitive, since several consecutive reduction and oxidation cycles could be applied without observing apparent degradation of the switch (Fig. 7d).

In contrast to **4** and **5**, compound **6** should present an additional switching mechanism, which consists in the thermal control of the equilibrium between their interconverting tautomers **6b** and **6c**. ^{1}H NMR spectroscopy was employed to investigate the temperature dependence of this process in acetonitrile, since the concentration ratio between these two isomers within the thermal range 238-308 K could be directly obtained from the analysis of their low field resonances: (a) the signal at $\delta \sim 8.20$ ppm, which corresponds to the two equivalent cyclohexadienyl protons of **6b**; (b) the signals at δ 8.40-8.60 ppm arising from the two aromatic protons of **6a**, which are equivalent at T > 288 K but become anisochronous when cooling, probably due to the hindered rotation of the bulky urea group (Fig. S8). From the integrals of these signals, the composition of the **6b-6c** equilibrium mixture and, therefore, the equilibrium constant of the tautomerization process ($K_{eq,\textbf{6b-6c}}$) could be determined at each temperature (Fig. 8a and Table S1). In this way we could confirm that the stability of the spirocyclic structure of the neutral state of **6** significantly decreases with temperature, as previously reported for analogous switch **2** [20]. In particular, **6b** relative concentration in this state of the switch varies from 15% at 238 K down to 5% at 308 K, a behavior that was found to be fully reversible upon repetitive warming-cooling cycles (Fig. 8a).

At temperatures higher than 308 K, the ^{1}H NMR signals of **6b** disappeared in the spectrum, which we ascribed to the combination of two different factors: (a) the low concentration expected for this compound in the **6b-6c** equilibrium mixture at these conditions, which should fall below the detection limit of the technique; (b) the increased thermal rate of interconversion between the two tautomers, which should make their ^{1}H NMR signals coalesce and be no longer resolvable. Actually, the effect of the interconversion rate on the ^{1}H NMR spectra was already observed at lower temperatures (288-308 K), where a clear broadening of the line width of the **6b** resonance at $\delta \sim 8.20$ ppm could be appreciated (Fig. S8). For these reasons, we used UV-vis absorption spectroscopy to estimate the decrement of the concentration of **6b** in the equilibrium mixture of tautomers at T > 308 K. As observed in Fig. 8b, the intensity of the visible band in the absorption spectrum of **6b-6c** dramatically diminished with temperature. Although thermal variation of the extinction coefficient of the cyclohexadienyl anion

chromophore may also play a role according to **6a** data (Fig. S9), the main reason behind this behavior is the reduction of the molar fraction of optically-active **6b** tautomer when temperature rises. Actually, when correcting for the thermal decrement of ε measured for **6a**, the relative concentration of **6b** in the **6b-6c** equilibrium mixture in acetonitrile at T = 336 K was estimated to be as low as 2.4% from the absorption data collected (Fig. 8a and Table S1).
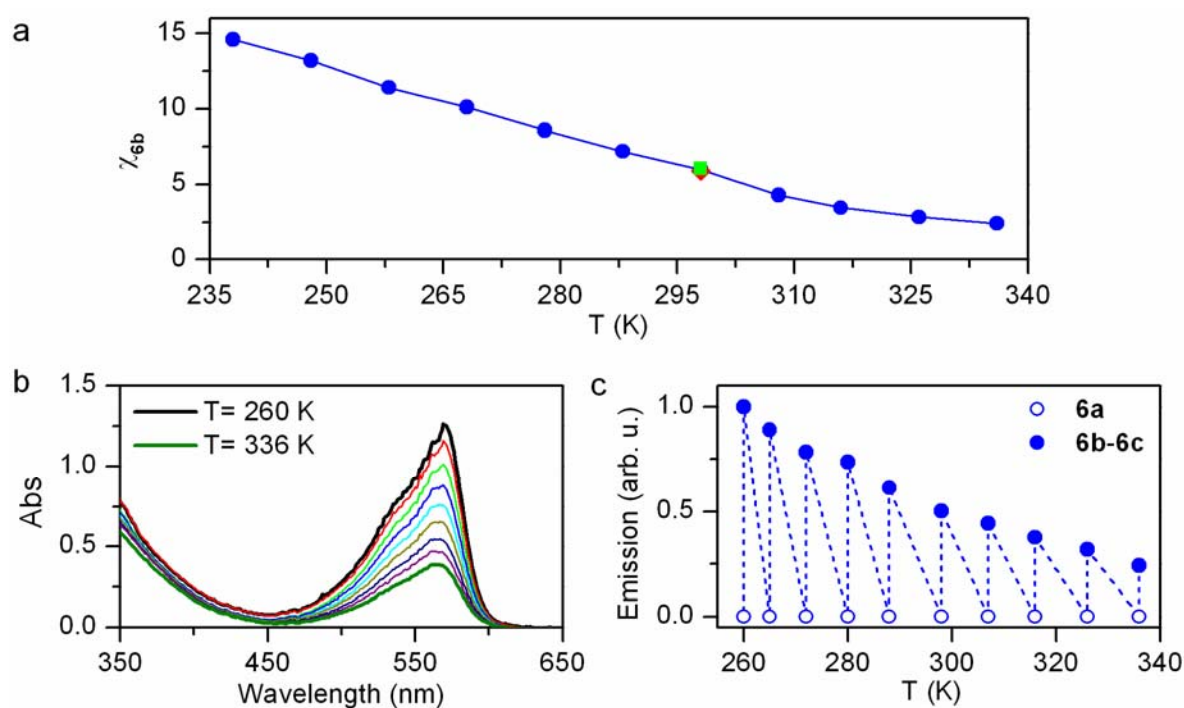
Fig. 8. (a) Temperature dependence of the molar fraction of **6b** in the neutral state of **6** in acetonitrile from NMR (238-308 K) and UV-Vis (318-336 K) data. Red and green dots indicate the χ_{6b} value at 298 K determined for the same sample after conducting one and two complete thermal cycles, respectively. (b) Temperature dependence of the UV-vis absorption spectrum of an acetonitrile solution of **6b-6c**. (c) Temperature dependence of the emission intensity of the *on* (**6b-6c**) and *off* (**6a**) states of compound **6** in acetonitrile.

Taking advantage of the temperature control of the **6b-6c** equilibrium and the different optical properties of both isomers, the performance of SZMC fluorescence switch **6** could be modulated by means of thermal

27

stimuli. This is illustrated in Fig. 8c, which plots the variation with temperature of the emission intensity of the *on* and *off* states of this compound in acetonitrile. Interestingly, the *on-off* fluorescence response of the system undergoes a 313% increase when cooling down from 336 K to 260 K. As such, **6** acts as a multi-addressable fluorescence switch capable to respond to chemical, electrochemical and thermal external signals. Although this behavior has already been reported for analogous compound **2** bearing isopropyl groups, replacement of these substituents by cyclohexyl groups in **6** allows modifying the stability of the emissive spirocyclic state of this type of compounds and, therefore, the range of temperatures at which maximum thermal modulation of the fluorescence switch operation is attained. In particular, because of the larger steric hindrance imparted by these cyclohexyl substituents, **6** would be better suited for applications where thermal control of *on-off* fluorescence response is required at very low temperatures.

CONCLUSIONS

By exploiting a simple one-pot synthetic methodology, new fluorescent switches based on stable spirocyclic zwitterionic Meisenheimer compounds were prepared, the substituents of which were tuned in order to optimize their optical response to external stimuli. Careful analysis of this synthetic strategy demonstrated that the formation of the desired spirocyclic structures is favored by the use of extremely electron-poor aromatic alcohols (in our case, picric acid and 2,6-dinitro-4-(trifluoromethyl)phenol) together with *N,N'*-carbodiimides bearing low steric hindrance alkyl groups (in our case, *N,N'*-dicyclohexylcarbodiimide and *N,N'*-diisopropylcarbodiimide). Moreover, the addition of a mixture of different carbodiimides allowed for the synthesis of new SZMC switches bearing a combination of distinct alkyl groups in their triazene ring. In this way, three novel fluorescent spirocyclic compounds could be synthesized that display halo-, electro- (**4** and **5**) and even thermochromic behavior (**6**). While the latter was achieved by replacing one nitro substituent by a trifluoromethyl group in the cyclohexadienyl anion chromophore of these systems, the nature of the alkyl groups introduced in the nearby triazene ring were found to critically influence: (a) the absorptivity and fluorescence quantum yield of the SZMC switches, which were maximized with cyclohexyl substituents; (b) their thermal response, which depends on the

steric hindrance effect imparted by these substituents on the stability of the spirocyclic structure of the system; (c) the interaction of the guanidine group with weak bases such as cyanide anions, which ultimately controls the sensitivity for the optical detection of such chemical analytes. Therefore, this demonstrates that appropriate choice of the substituents in SZMC fluorescent switches is a crucial step when designing the use of these smart molecules in selected applications.

ACKNOWLEDGMENTS

REFERENCES

[1]   Zhao Y, Yu S, Sun W, Liu L, Lu J, McEachern D, et al. A potent small-molecule inhibitor of the MDM2-p53 interaction (MI-888) achieved complete and durable tumor regression in mice. J Med Chem 2013;56:5553–61. doi:10.1021/jm4005708.

[2]   Zheng Y, Tice CM, Singh SB. The use of spirocyclic scaffolds in drug discovery. Bioorganic Med Chem Lett 2014;24:3673–82. doi:10.1016/j.bmcl.2014.06.081.

[3]   Tömböly C, Ballet S, Feytens D, Köver KE, Borics A, Lovas S, et al. Endomorphin-2 with a β-turn backbone constraint retains the potent μ-opioid receptor agonist properties. J Med Chem 2008;51:173–7. doi:10.1021/jm7010222.

[4]   Pudzich R, Fuhrmann-Lieker T, Salbeck J. Spiro compounds for organic electroluminescence and related applications. Adv Polym Sci 2006;199:83–142. doi:10.1007/12_074.

[5]   Lukyanov BS, Metelitsa A V, Voloshin NA, Alexeenko YS, Lukyanova MB, Vasilyuk GT, et al. Solid state photochromism of spiropyrans. Int J Photoenergy 2005;7:17–22. doi:10.1155/S1110662X05000036.

[6]   Berkovic G, Krongauz V, Weiss V. Spiropyrans and Spirooxazines for Memories and Switches. Chem Rev 2000. doi:10.1021/cr9800715.

[7]   Klajn R. Spiropyran-based dynamic materials. Chem Soc Rev 2014;43:148–84.

doi:10.1039/C3CS60181A.

[8] Shiraishi Y, Shirakawa E, Tanaka K, Sakamoto H, Ichikawa S, Hirai T. Spiropyran-Modified Gold Nanoparticles: Reversible Size Control of Aggregates by UV and Visible Light Irradiations. ACS Appl Mater Interfaces 2014;6:7554–62. doi:10.1021/am5009002.

[9] Ueda M, Kim H-B, Ichimura K. Photocontrol of dispersibility of colloidal silica. Mater Lett 1994;20:245–9. doi:10.1016/0167-577X(94)90094-9.

[10] Tong R, Hemmati HD, Langer R, Kohane DS. Photoswitchable nanoparticles for triggered tissue penetration and drug delivery. J Am Chem Soc 2012;134:8848–55. doi:10.1021/ja211888a.

[11] Shi W, Ma H. Rhodamine B thiolactone: a simple chemosensor for Hg2+ in aqueous media. Chem Commun 2008:1856–8. doi:10.1039/b717718f.

[12] Al-Kaysi R, Creed D, Valente E. Meisenheimer complex from picric acid and diisopropylcarbodiimide. J Chem Crystallogr 2004;34:685–92. doi:1074-1542/04/1000-0685.

[13] Al-Kaysi RO, Guirado G, Valente EJ. Synthesis and Characterization of a New Fluorescent Zwitterionic Spirocyclic Meisenheimer Complex of 1,3,5-Trinitrobenzene. European J Org Chem 2004;2004:3408–11. doi:10.1002/ejoc.200400260.

[14] Al-Kaysi RO, Gallardo I, Guirado G. Stable Spirocyclic Meisenheimer Complexes. Molecules 2008;13:1282–302. doi:10.3390/molecules13061282.

[15] Al-Kaysi RO, Bourdelande JL, Gallardo I, Guirado G, Hernando J. Investigation of an Acid–Base and Redox Molecular Switch: From Bulk to the Single-Molecule Level. Chem - A Eur J 2007;13:7066–74. doi:10.1002/chem.200700236.

[16] Gallardo I, Guirado G. Electrochemical mechanism of spiro and zwitterionic Meisenheimer compounds: A potential fluorescence molecular switching system. Electrochem Commun 2007;9:173–9. doi:10.1016/j.elecom.2006.08.054.

[17] Kirk KL, Cohen LA, Yeager E, Sachs T, Hovorka F, Jones RR, et al. Spiro Meisenheimer Complexes from 1978;43:3578–84.

[18] Buck P. Reactions of Aromatic Nitro Compounds with Bases. Angew Chemie Int Ed English 1969;8:120–31. doi:10.1002/anie.196901201.

[19] Gallardo I, Guirado G. Electrochemical mechanism of spiro and zwitterionic Meisenheimer compounds: A potential fluorescence molecular switching system. Electrochem Commun 2007;9:173–9. doi:10.1016/j.elecom.2006.08.054.

[20] Gallardo I, Guirado G, Hernando J, Morais S, Prats G. A multi-stimuli responsive switch as a fluorescent molecular analogue of transistors. Chem Sci 2016;7:1819–25. doi:10.1039/C5SC03395K.

[21] Al-Kaysi RO, Müller AM, Ahn T, Lee S, Bardeen CJ. Effects of sonication on the size and crystallinity of stable zwitterionic organic nanoparticles formed by reprecipitation in water. Langmuir 2005;21:7990–4. doi:10.1021/la051183b.

[22] Benet M, Villabona M, Llavina C, Mena S, Hernando J, Al-Kaysi RO, et al. Fluorescent "Turn-Off" Detection of Fluoride and Cyanide Ions Using Zwitterionic Spirocyclic Meisenheimer Compounds. Molecules 2017;22:1842.

[23] Das T, Haldar D. Mopping up the oil, metal, and fluoride ions from water. ACS Omega 2017;2:6878–87. doi:10.1021/acsomega.7b01379.

[24] Das T, Pramanik A, Haldar D. On-line Ammonia Sensor and Invisible Security Ink by Fluorescent Zwitterionic Spirocyclic Meisenheimer Complex. Sci Rep 2017;7:40465. doi:10.1038/srep40465.

[25] Dasary SSR, Singh AK, Lee KS, Yu H, Ray PC. A miniaturized fiber-optic fluorescence analyzer for detection of Picric-acid explosive from commercial and environmental samples. Sensors Actuators B Chem 2018;255:1646–54. doi:10.1016/j.snb.2017.08.175.

[26] Kircher T, Lohmannsroben HG. Photoinduced charge recombination reactions of a perylene dye in acetonitrile. Phys Chem Chem Phys 1999;1:3987–92. doi:10.1039/A902356I.

[27] Sánchez RS, Gras-Charles R, Bourdelande JL, Guirado G, Hernando J. Light- and redox-controlled fluorescent switch based on a perylenediimide-dithienylethene dyad. J Phys Chem C 2012;116:7164–72. doi:10.1021/jp300815p.

[28] Stevens WC, Hill DC. General methods for flash chromatography using disposable columns. Mol Divers 2009;13:247–52. doi:10.1007/s11030-008-9104-x.

[29] Still C. Flash chromatography. Mater Today 2002;5:42. doi:10.1016/S1369-7021(02)01160-4.

Supplementary Material

New Smart Functional Fluorophores based on

Spirocyclic Zwitterionic Meisenheimer Complexes

Neus Sala,[a] Gemma Prats,[a,] Marc Villabona,[a] Iluminada Gallardo,[a] Tarafah Hamdan, [b]

Rabih O. Al-Kaysi,*[b] Jordi Hernando,*[a] and Gonzalo Guirado*[a]

[a] Departament de Química, Universitat Autònoma de Barcelona, 08193 Cerdanyola del Vallès, Spain

[b] College of Science and Health Professions-3124, King Saud bin Abdulaziz University for Health Sciences/ King Abdullah International Medical Research Center, Ministry of National Guard Health Affairs, Riyadh 11426, Kingdom of Saudi Arabia

E-mails of corresponding authors: jordi.hernando@uab.cat (J.H.); rabihalkaysi@gmail.com and

kaysir@ksau-hs.edu.sa (R.O.K.); gonzalo.guirado@uab.cat (G.G.)
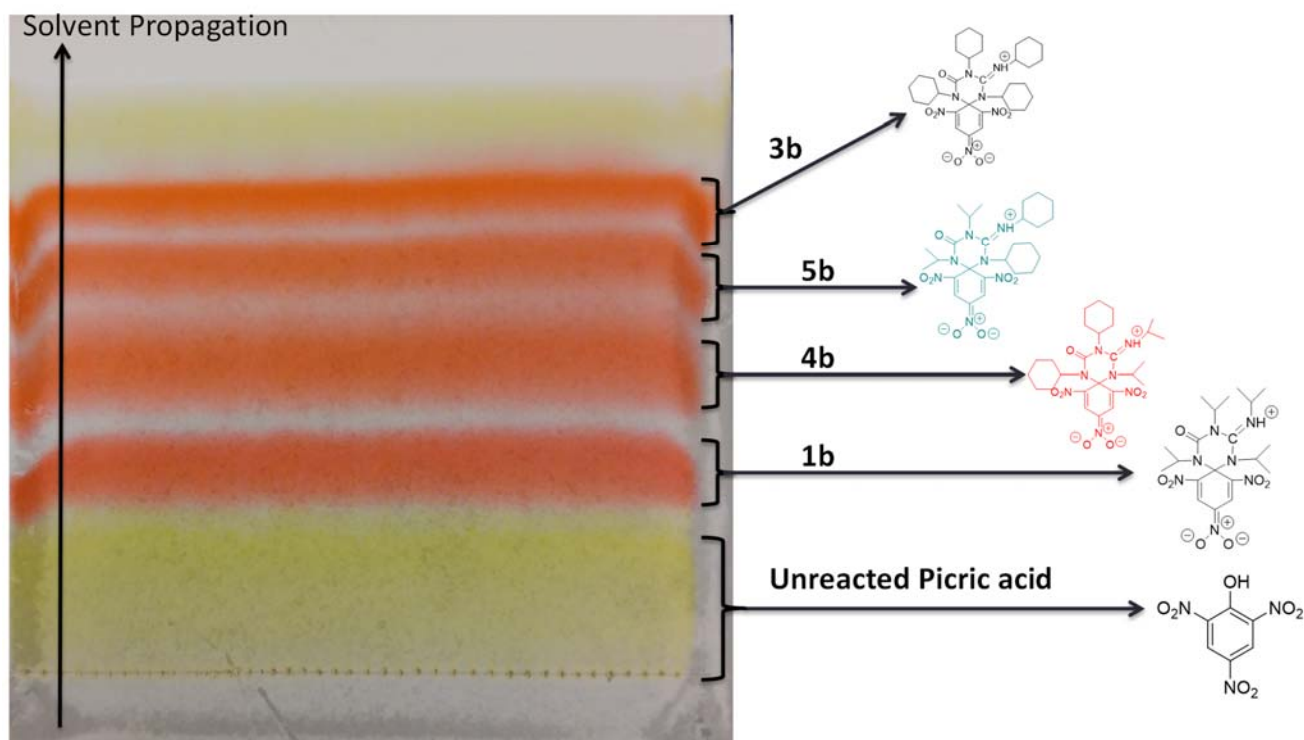
Fig. S1: Preparative TLC of the crude mixture obtained during the synthesis of SZMC switches **4b** and **5b** (silica gel, ethyl acetate:hexane). The separation of four different orange-colored products could be appreciated by naked eye, which were identified by means of NMR and HR-MS as compounds **3b**, **5b**, **4b** and **1b**. Yellow-colored compounds corresponded to monosubstitution products **7** and **8** (upper band) and unreacted picric acid (lower band).
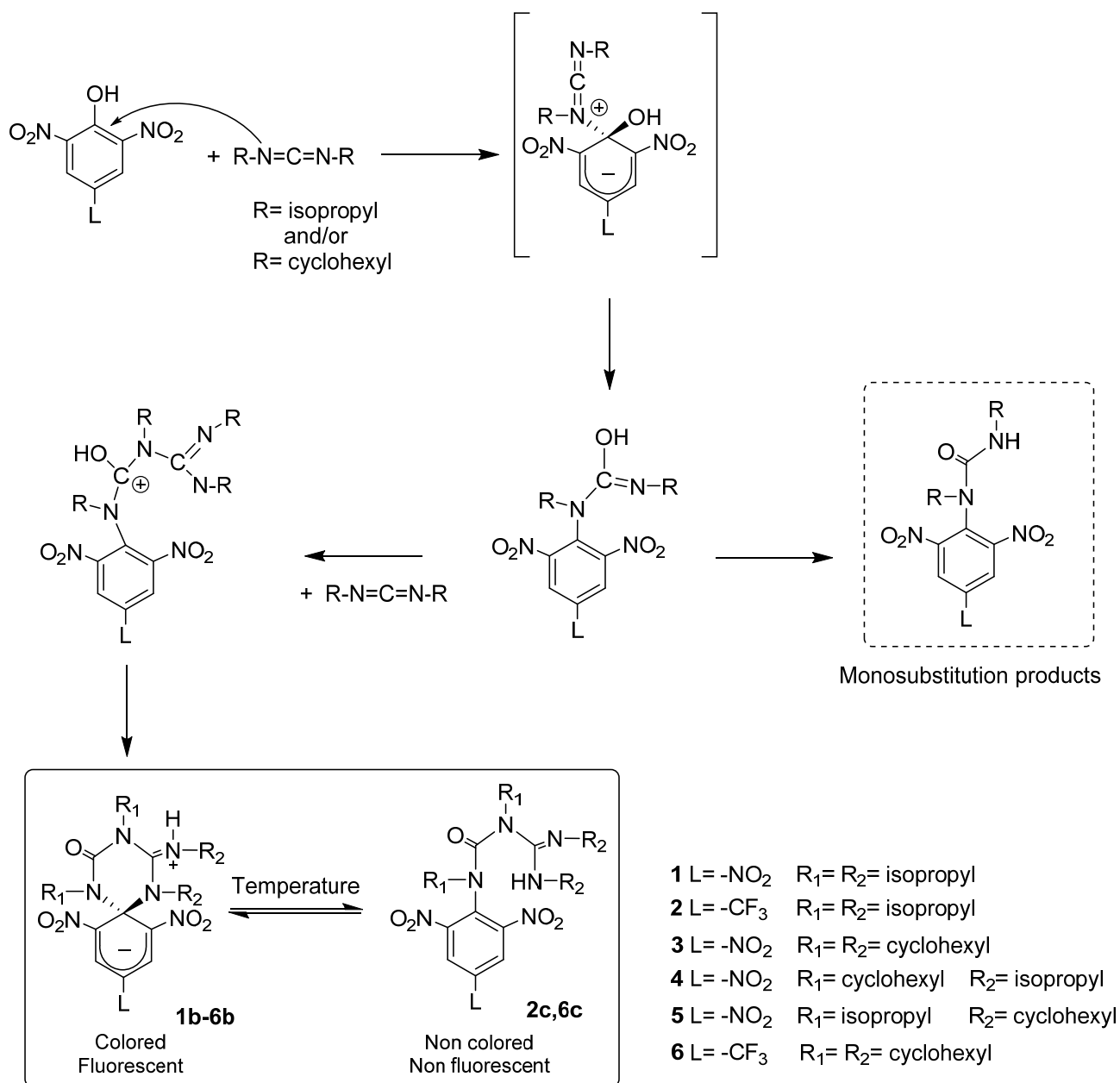
Scheme S1: Plausible reaction mechanism for the formation of SZMC switches.
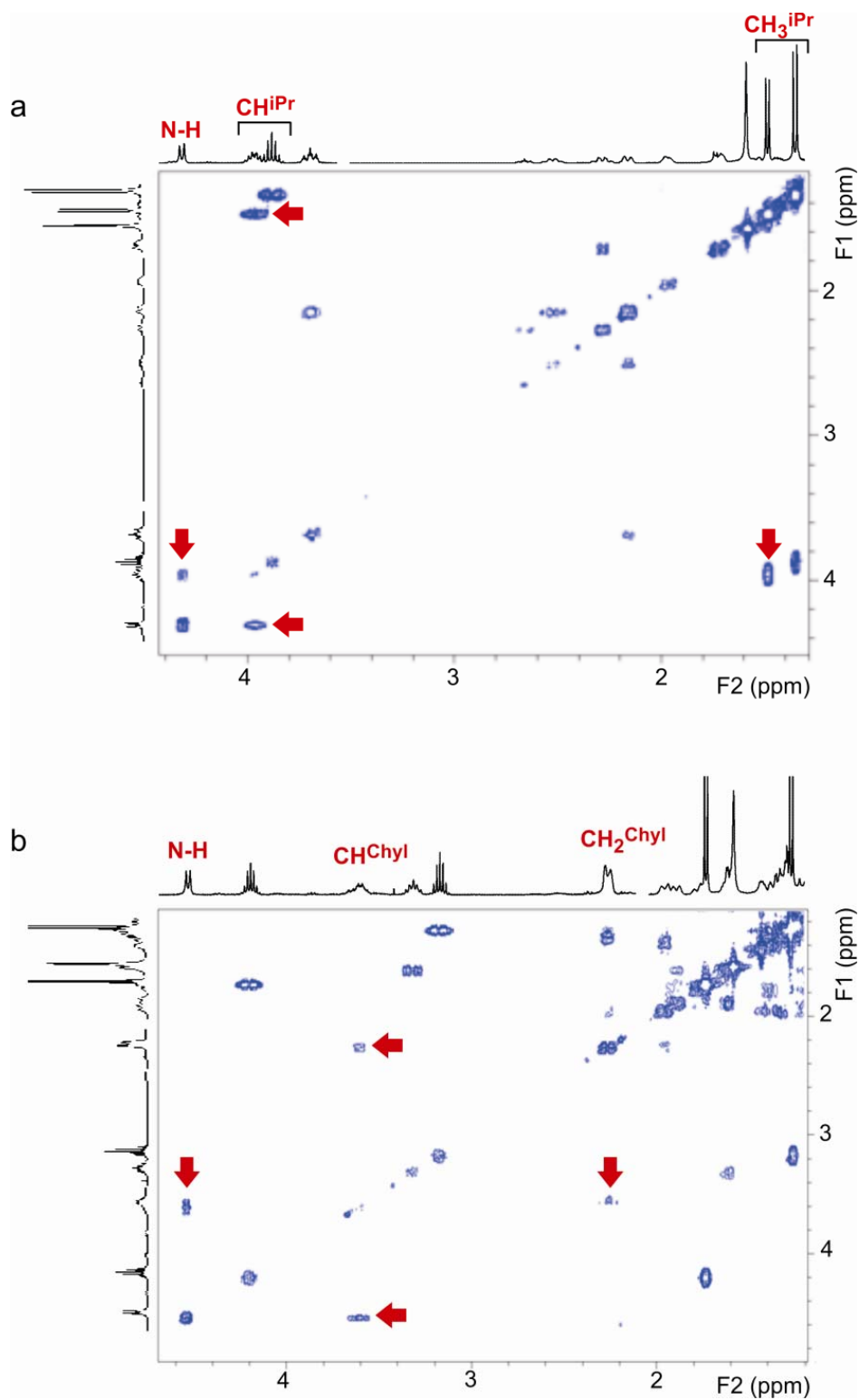
Fig. S2: COSY spectra (400 MHz, CDCl₃) of (a) **4b** and (b) **5b**. In the case of **4b**, cross-peaks are observed between one of the CH multiplets at δ 3.93 ppm (CH^iPr) and both the NH resonance at δ 4.30 ppm and one of the isopropyl CH₃ doublets at δ 1.47 ppm (CH₃^iPr). By the contrary, cross-correlation is observed

in the spectrum of **5b** between one of the CH multiplets at δ 3.61 ppm (CH^{Chxyl}) and both the NH resonance at δ 4.53 ppm and one of the cyclohexyl CH$_2$ signals at δ 2.25 ppm (CH$_2$^{Chxyl}). For sake of clarity, the intensity of the 1D ^{1}H NMR signals in the region 4.2 – 3.6 ppm (for **4b**) and 4.6 – 2.1 ppm (for **5b**) were amplified (x3).
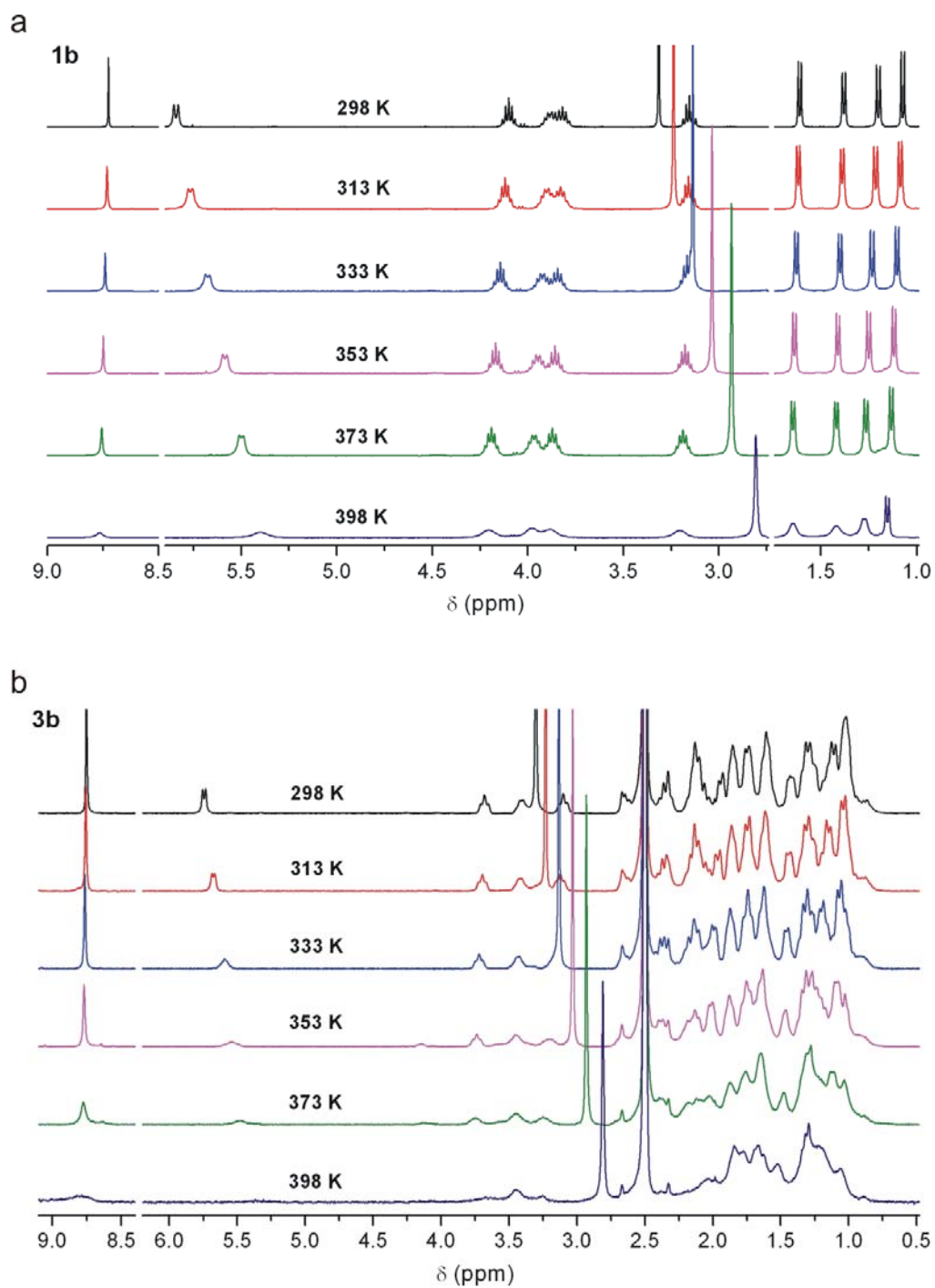
Fig. S3: Thermal dependence of the ^{1}H NMR (400 MHz, DMSO-d$_6$) spectra of (a) **1b** and (b) **3b**. For sake of clarity, the intensity of the ^{1}H NMR signals in the region 5.9 – 2.7 ppm of (a) was amplified (x5).
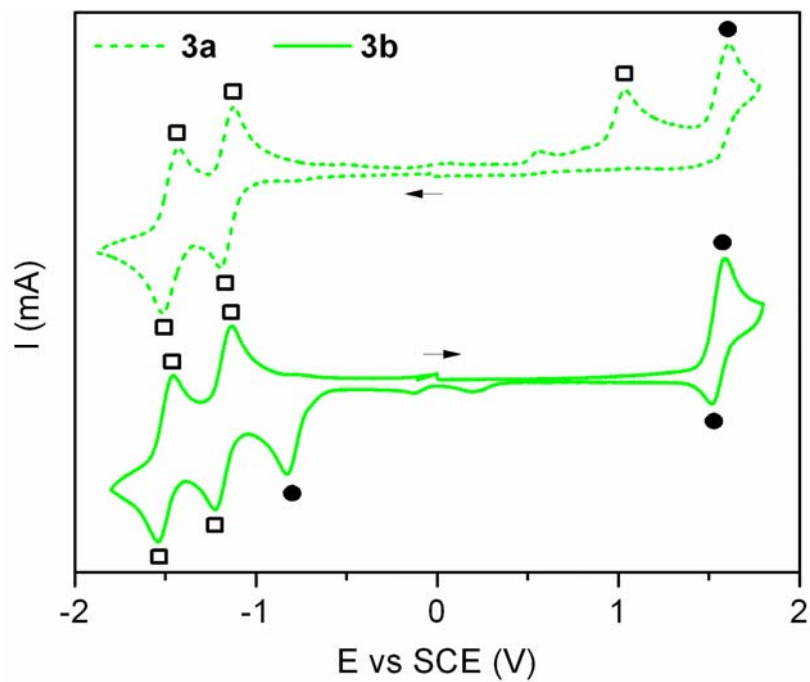
Fig. S4: Cyclic voltammograms of **3a** and **3b** in acetonitrile at 298 K ($c = 5.0 \times 10^{-4}$ M, 0.1 M n-Bu$_4$NPF$_6$, scan rate = 0.5 V s^{-1}). Solid circles and hollow squares are used to assign the electrochemical waves arising from the anionic and neutral states of these compounds, respectively. Arrows indicate the direction of the potential scan in each case.
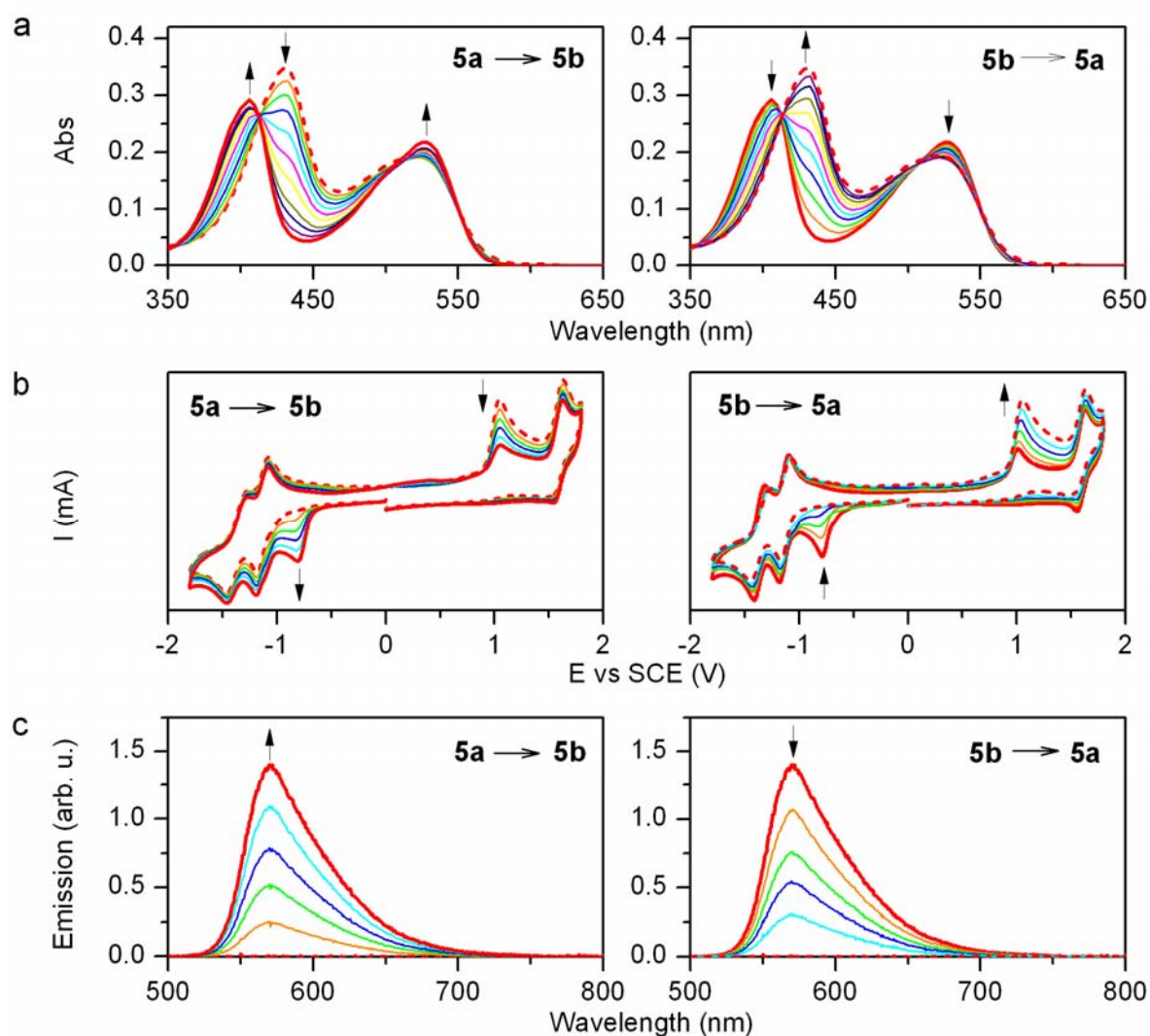
Fig. S5: Acid-base interconversion between **5a** and **5b** monitored by (a) UV-vis absorption spectroscopy (c = 2.0x10^{-5} M, acetonitrile, 298 K), (b) cyclic voltammetry (c = 2.0x10^{-3} M, acetonitrile + 0.1 M *n*-Bu$_4$NPF$_6$, scan rate 0.5 V s^{-1}, 298 K), and (c) fluorescence spectroscopy (c = 1.0x10^{-5} M, acetonitrile, λ_{exc}= 473 nm, 298 K). In each case increasing amounts of HClO$_4$ or TBAOH were added until reaching *ca*. 1 equivalent of acid or base.
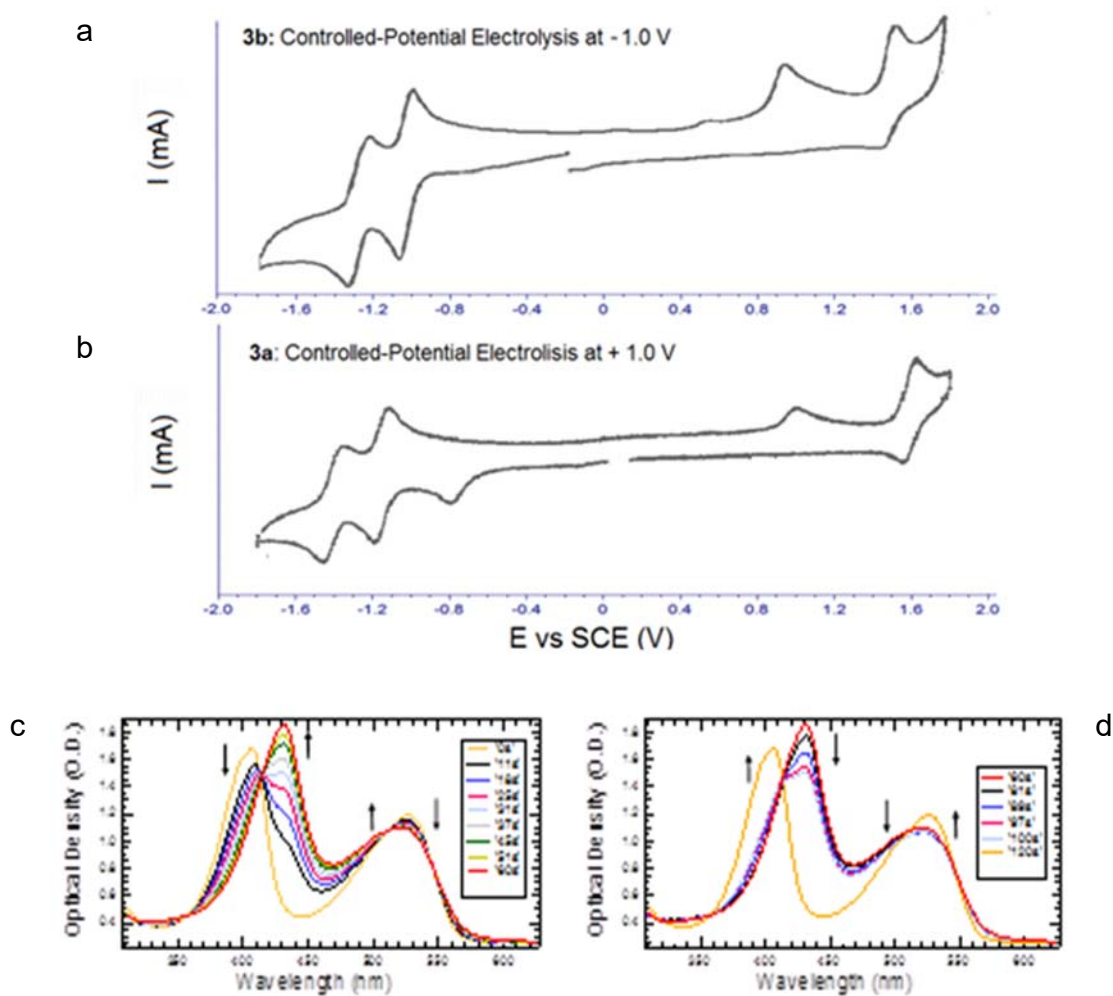
Fig. S6: (a) Cyclic voltammogram after reduction of **3b** in acetonitrile at E = -1.0 V (vs SCE) and 1.25 F (c = 5.0x10^{-3} M, 0.1 M n-Bu$_4$NPF$_6$, scan rate = 0.5 V s^{-1}). (b) Cyclic voltammogram after oxidation of **3a** in acetonitrile at E = +1.0 V (vs SCE) and 1.25 F (c = 5.0x10^{-3} M, 0.1 M n-Bu$_4$NPF$_6$, scan rate = 0.5 V s^{-1}). (c) Spectroelectrochemical measurements of the redox interconversion **3b** → **3a** when applying E = -1.0 V (vs SCE) during 60 s to a 1.2x10^{-3} M solution of **3b** in acetonitrile. (d) Spectroelectrochemical measurements of the redox interconversion **3a** → **3b** when applying E = +1.0 V (vs SCE) during 60 s to a 1.2x10^{-3} M solution of **3a** in acetonitrile.
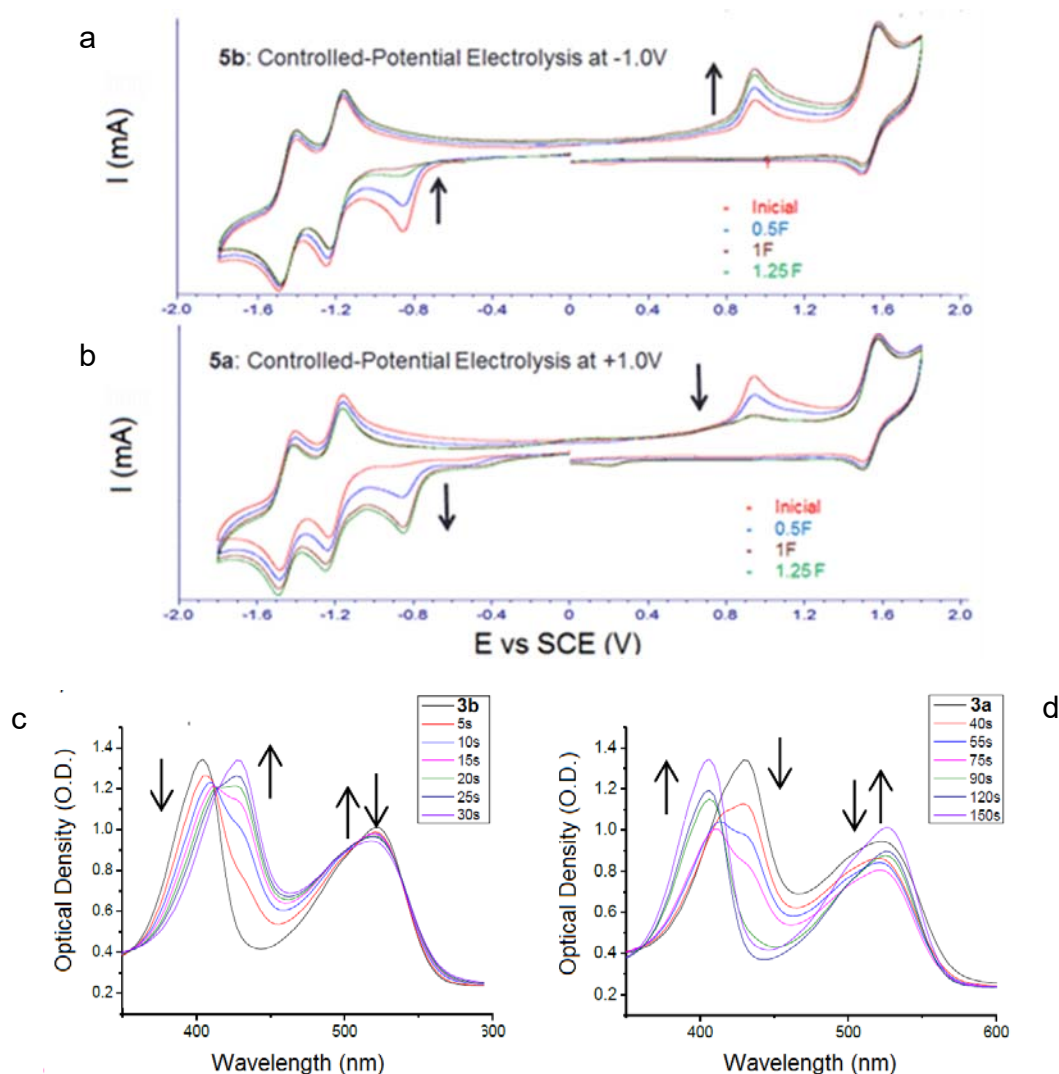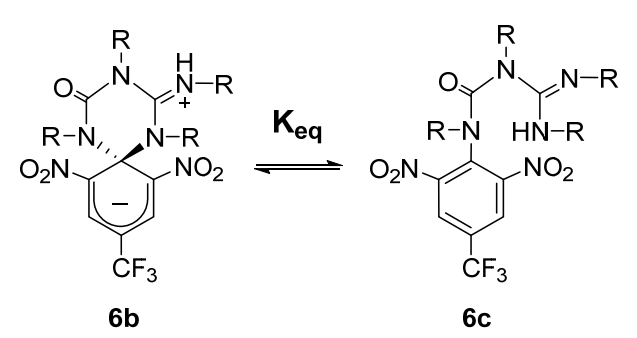
Fig. S7: (a) Cyclic voltammogram after reduction of **5b** in acetonitrile at E = -1.0 V (vs SCE) and 1.25 F (c = 4.0x10^{-3} M, 0.1 M n-Bu$_4$NPF$_6$, scan rate = 0.5 V s^{-1}). (b) Cyclic voltammogram after oxidation of **5a** in acetonitrile at E = +1.0 V (vs SCE) and 1.25 F (c = 4.0x10^{-3} M, 0.1 M n-Bu$_4$NPF$_6$, scan rate = 0.5 V s^{-1}). (c) Spectroelectrochemical measurements of the redox interconversion **5b** $\rightarrow$ **5a** when applying E = -1.0 V (vs SCE) during 30 s to a 1.2x10^{-3} M solution of **5b** in acetonitrile. (d) Spectroelectrochemical measurements of the redox interconversion **5a** $\rightarrow$ **5b** when applying E = +1.0 V (vs SCE) during 150 s to a 1.2x10^{-3} M solution of **5a** in acetonitrile.
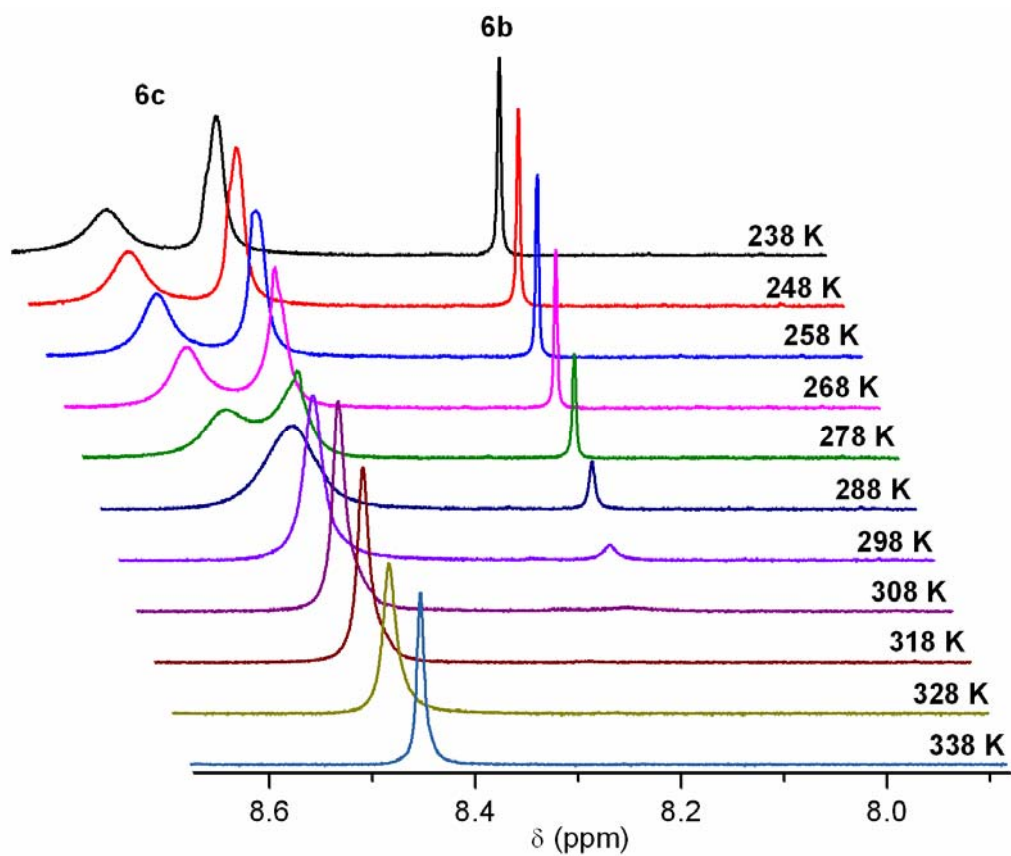
Fig. S8. Variation of the low-field signals of the ^{1}H NMR spectrum (400 MHz, CD$_3$CN) of an equilibrium mixture of **6b** and **6c** with temperature. The signal at δ~8.20 ppm corresponds to the cyclohexadienyl protons of **6b**, whereas the signals at δ 8.60-8.40 ppm arise from the aromatic nuclei of **6c**.

Table S1. Variation of the equilibrium constant of the **6b-6c** tautomer equilibrium with temperature.[a]

T (K)	K_{eq}[a]
238	5.8
248	6.6
258	7.8
268	8.9
278	10.6
288	12.9
298	15.7
308	23.4
316	27.9
326	34.1
336	----

[a] In acetonitrile. Values derived from the analysis of the low field region of the ^1H NMR spectrum of the tautomer mixture (238-308 K) and from the temperature dependence of its absorption spectra (316-336 K).
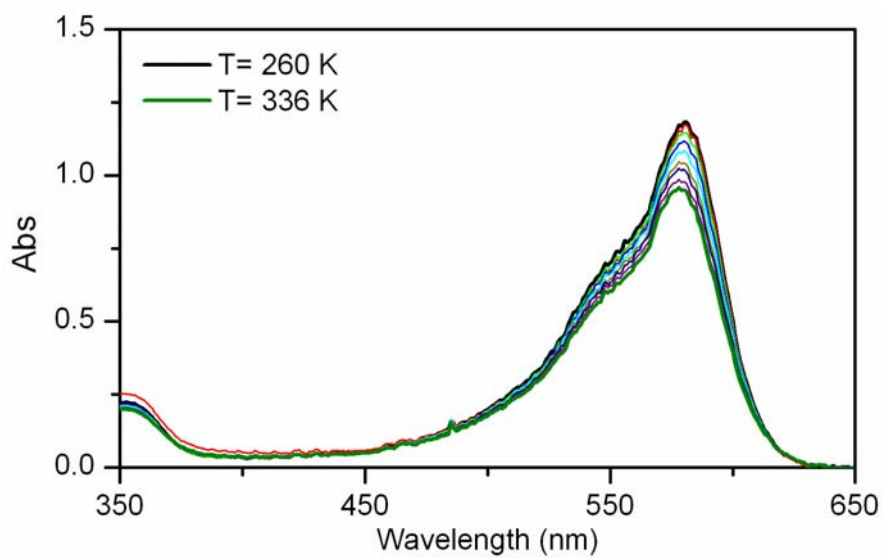
Fig. S9: Temperature dependence of the UV-vis absorption spectrum of an acetonitrile solution of **6a** from 260 K to 336 K ($c = 7.3 \times 10^{-5}$ M).